

**Document Version**

Final published version

**Licence**

CC BY

**Citation (APA)**

Avallone, F., Bosia, F., Chen, Y., Colombo, G., Craster, R., De Ponti, J. M., Kotsonis, M., Michelis, T., Ragni, D., & More Authors (2026). Metamaterials and Fluid Flows. *Nature Communications*, 17(1), Article 4144.  
<https://doi.org/10.1038/s41467-026-70163-2>

**Important note**

To cite this publication, please use the final published version (if applicable).  
Please check the document version above.

**Copyright**

In case the licence states “Dutch Copyright Act (Article 25fa)”, this publication was made available Green Open Access via the TU Delft Institutional Repository pursuant to Dutch Copyright Act (Article 25fa, the Taverne amendment). This provision does not affect copyright ownership.  
Unless copyright is transferred by contract or statute, it remains with the copyright holder.

**Sharing and reuse**

Other than for strictly personal use, it is not permitted to download, forward or distribute the text or part of it, without the consent of the author(s) and/or copyright holder(s), unless the work is under an open content license such as Creative Commons.

**Takedown policy**

Please contact us and provide details if you believe this document breaches copyrights.  
We will remove access to the work immediately and investigate your claim.

# Metamaterials and Fluid Flows

---

Received: 3 September 2025


---

Accepted: 20 February 2026

---

Published online: 04 March 2026

---

 Check for updates

---

Francesco Avallone<sup>1</sup>, Federico Bosia<sup>2</sup>, Yi Chen<sup>3</sup>, Giada Colombo<sup>4</sup>, Richard Craster<sup>5</sup>, Jacopo Maria De Ponti<sup>6</sup>, Nicolò Fabbiane<sup>7</sup>, Michael R. Haberman<sup>8</sup>, Mahmoud I. Hussein<sup>9</sup>, Wontae Hwang<sup>10</sup>, Umberto Iemma<sup>4</sup>, Abigail Juhl<sup>11</sup>, Muamer Kadic<sup>12</sup>✉, Marios Kotsonis<sup>13</sup>, Vincent Laude<sup>12</sup>, Olivier Marquet<sup>14</sup>, Fabien Mery<sup>15</sup>, Theodoros Michelis<sup>13</sup>, Mostafa Nouh<sup>16</sup>, Daniele Ragni<sup>13</sup>, Marie Touboul<sup>17</sup>, Martin Wegener<sup>3</sup> & Anastasiia O. Krushynska<sup>18</sup>✉

---

Understanding and controlling the dynamic interactions between fluid flows and solid materials and structures—a field known as fluid-structure interaction—is central not only to established disciplines such as aerospace and naval engineering, but also to emerging technologies such as energy harvesting, soft robotics, and biomedical devices. In recent years, the advent of metamaterials has provided exciting opportunities to rethink and redesign fluid-structure interactions. The idea of engineering the internal structure of materials that interface with fluid flows opens a new horizon for the precise and effective manipulation and control of coupled fluidic, acoustic, and elastodynamic responses. This review focuses on this relatively unexplored interdisciplinary theme with broad technological significance. Salient potential applications, such as reduction of fuel consumption in transport systems, efficiency of renewable energy extraction, noise mitigation, and resilience against structural fatigue, depend on controlling interactions among flow, acoustic, and vibration mechanisms. Flow control, for example, which spans a wealth of regimes such as laminar, transitional, turbulent, and unsteady separated flows, is strongly influenced by fluid-structure interaction. This review surveys and discusses conceptual frameworks that describe the interplay between fluids and elastic solids, with a focus on contemporary and emerging concepts. The paper is organised into three main sections: fluid-structure and flow-phonon interactions, flow-induced acoustic interactions with metamaterials, and exotic metamaterial concepts with potential impact on fluid-structure interaction. It concludes with perspectives on current challenges and future directions in this rapidly expanding area of research.

Dynamic interactions between fluid flows and solid structures underpin various natural phenomena that can be used for engineered systems. These fluid-structure interactions are central not only to traditional fields like aerospace and naval engineering but also to emerging technologies in energy harvesting, robotics, and biomedical devices. In recent years, the advent of metamaterials-composites

designed to exhibit effective properties that go beyond those of their constituents, and that are often unique and non-intuitive—has provided exciting opportunities to rethink and redesign such interactions. Architecting the topology of such functional materials enables the manipulation of mechanical, acoustic, and/or fluidic responses and offers new strategies for controlling the coupled fields.

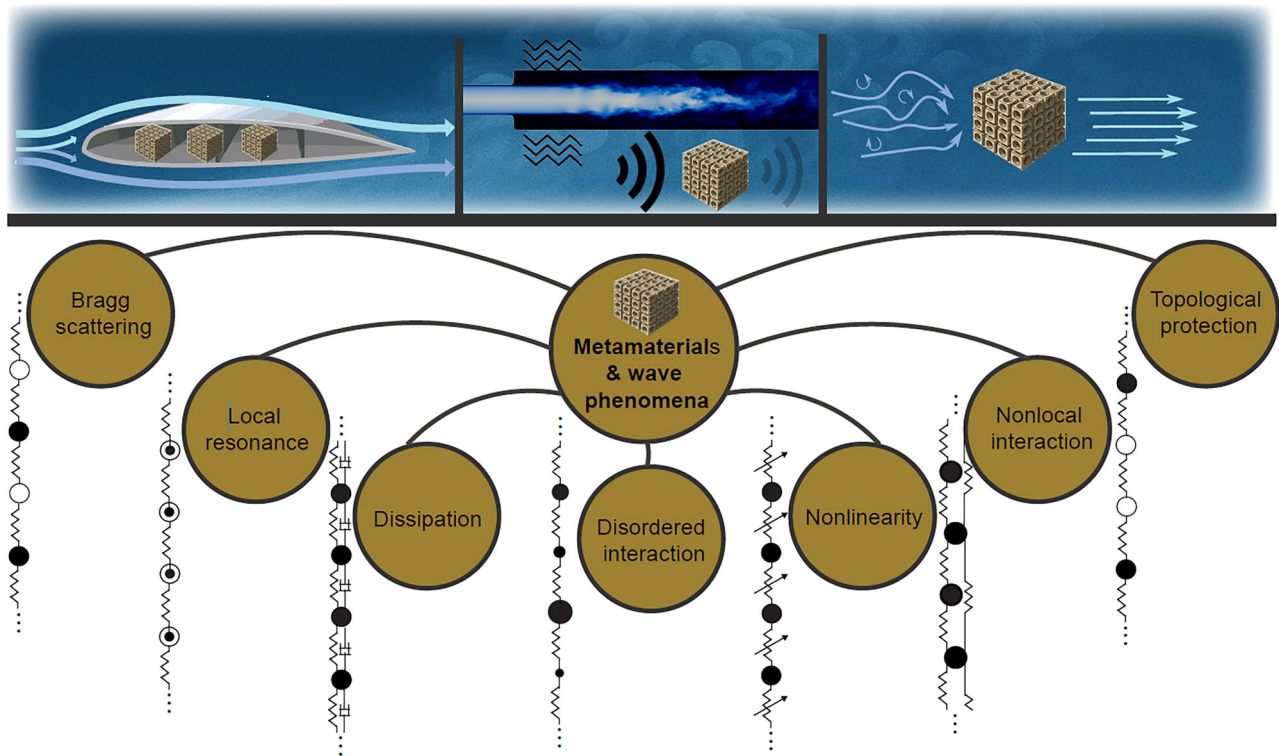


**Fig. 1 | Fluid-flow-induced phenomena and structural wave propagation mechanisms for flow control.** The top part illustrates fluid–structure interactions, flow-induced acoustics, and fluid flows through a structure together with

schematics of possible application scenarios involving metamaterials. The bottom part overviews wave manipulation mechanisms for engineered fluid–structure interactions.

This review summarizes an under-explored but critically important frontier: the interplay between metamaterials and various wave motion mechanisms that can be engineered at the material level, and fluid (i.e., gas and liquid) flows—as conceptualized in Fig. 1. This focus addresses engineering challenges where controlling or exploiting fluid–structure interaction can dramatically improve performance. Consider, for instance, the hydrodynamic drag experienced by maritime vessels during long-distance travel. Viscous shear forces dictate a significant portion of the vessel’s fuel consumption at the hull–water interface. Similarly, in aeronautical applications, turbulent and/or unsteady airflow over a wing or an engine nacelle leads to energy losses, acoustic emissions, and structural fatigue. In both cases, tailoring the fluid–solid interface through specially designed surfaces and subsurfaces can offer substantial gains. Fluid–structure interactions are also critical in the context of flow-induced vibrations, where unstable flow patterns can excite resonant structural modes, leading to fatigue or functional failure, or, conversely, can be used for energy harvesting. Moreover, acoustic metamaterials enable precise manipulation of sound waves in elastic solids, fluids and gases, offering new strategies for vibration damping, noise control, and wave manipulation. These interactions are inherently multiphysical and multiscale, requiring a combination of fluid dynamics, elasticity, acoustics, and interface phenomena.

To provide a comprehensive approach to this interdisciplinary domain, this review is hierarchically structured into three key application areas that illustrate the potential influence of engineered surfaces and subsurfaces, including various classes of metamaterials, on fluid–structure interaction systems:

- *Flow–structure interactions.* This section examines how the geometry and material properties of structured materials, or patterned surfaces and subsurfaces, can control the behavior of transitional boundary layers, the suppression of turbulence, and the dissipation of energy in internal and external flows. The

prospects of metamaterials in manipulating surface gravity waves in liquid flows are also considered.

- *Flow-induced acoustic interactions with metamaterials.* This section discusses how metamaterials and phononic crystals can manipulate sound generated by fluid flows, using mechanisms such as local resonance, Bragg scattering, and anisotropic impedance. These concepts are vital for aeroacoustic design and noise mitigation, especially in high-speed flow regimes. The potential of metamaterials in the manipulation of micro- and nano-particles by sound waves is also described.
- *Exotic metamaterial concepts in fluid–structure interaction.* This section overviews how notable functionalities or properties of metamaterials, including topologically protected states, nonlocal elasticity, and temporal or spatiotemporal varying properties, can potentially be used to enhance wave control in flow environments. An outlook is provided on how these distinctive metamaterials can open new possibilities and degrees of freedom in flow control by going beyond rigid-wall assumptions and the limits of Cauchy elasticity.

These three key application and concept areas are illustrated in Fig. 1. The schematics of the flow- and sound–structure interactions have direct counterparts in real-world contexts. For instance, aircraft wings interact dynamically with surrounding airflow, which influences lift, drag, and structural response, providing a classic example of coupled flow–structure interactions. In addition, the aircraft engine inlets are sites of complex flow patterns that couple with rotating and stationary components. These interactions are crucial in determining aircraft performance, fuel efficiency, and resilience to structural fatigue.

These examples illustrate the need for advanced theoretical and computational tools capable of describing and predicting fluid–structure interactions. The following sections present concepts

Gas	Gas / Fluid	Fluid
$\nabla \cdot \left[ \frac{1}{\rho_g} \nabla p \right] = \frac{1}{B_g} \frac{\partial^2 p}{\partial t^2}$ <p><math>\rho_g</math>: gas mass density  <math>p</math>: acoustic pressure  <math>B_g</math>: gas bulk modulus</p>	$\frac{1}{\rho_g} \nabla p \cdot \mathbf{n} = \mathbf{v} \cdot \mathbf{n}$ $-p\mathbf{n} = [\lambda_F(\nabla \cdot \mathbf{v}) - P]\mathbf{n} + [\mu_F(\nabla \mathbf{v} + \nabla \mathbf{v}^T)] \cdot \mathbf{n}$	$\frac{\partial \rho_F}{\partial t} + \nabla \cdot (\rho_F \mathbf{v}) = 0$ $\rho_F \left[ \frac{\partial \mathbf{v}}{\partial t} + \mathbf{v} \cdot \nabla \mathbf{v} \right] = -\nabla P + \nabla \cdot [\mu_F(\nabla \mathbf{v} + \nabla \mathbf{v}^T) + \lambda_F(\nabla \cdot \mathbf{v})\mathbf{I}] + \rho_F \mathbf{f}$ <p><math>\mu_F</math>: dynamic viscosity  <math>\lambda_F</math>: Second (bulk) viscosity  <math>\mathbf{f}</math>: external body force  <math>\mathbf{I}</math>: Identity tensor</p>
$\frac{1}{\rho_g} \nabla p \cdot \mathbf{n} = \frac{\partial^2 \mathbf{u}}{\partial t^2} \cdot \mathbf{n}$ $-p\mathbf{n} = \boldsymbol{\sigma} \cdot \mathbf{n}$	<p style="text-align: center;"><b>boundary conditions</b></p>	$\boldsymbol{\sigma} \cdot \mathbf{n} = [-P\mathbf{I} + \mu_F(\nabla \mathbf{v} + \nabla \mathbf{v}^T) + \lambda_F(\nabla \cdot \mathbf{v})\mathbf{I}] \cdot \mathbf{n}$ $\mathbf{v} = \frac{\partial \mathbf{u}}{\partial t}$
<p style="text-align: center;"><b>Solid</b></p> $\nabla \cdot \boldsymbol{\sigma} = \rho_s \frac{\partial^2 \mathbf{u}}{\partial t^2}, \quad \boldsymbol{\sigma} = \mathbf{C}_S : \frac{1}{2}(\nabla \mathbf{u} + \nabla \mathbf{u}^T)$ <p><math>\rho_s</math>: solid mass density    <math>\mathbf{u}</math>: displacement vector    <math>\boldsymbol{\sigma}</math>: stress tensor    <math>\mathbf{C}_S</math>: elasticity tensor</p>		

**Fig. 2 | Schematic representation of the theoretical formulation for fluid–structure interaction.** The three main dynamic equations for gas, fluid, and solid media, are shown together with interface boundary conditions for the three

different combinations. Note that phenomena discussed in this review can be adequately described by *linear* equations for structural dynamics. The symbol  $\mathbf{n}$  denotes the outward-pointing unit normal vector at a boundary or interface.

and theoretical frameworks rooted in continuum mechanics, fluid dynamics, acoustics, and materials science to model these rich and complex interfaces. Recent progress in fluid-flow control using engineered material and surface/subsurface topologies is reviewed, and the status of metamaterial research in the context of elastic, acoustic, and fluidic environments is discussed.

### Theoretical framework for fluid–structure interactions in metamaterials

Fluid–structure interaction lies at the core of many physical phenomena, from flow-induced drag on ship hulls to acoustic wave propagation in architected solids. Metamaterials enable novel control over such interactions but necessitate a deep understanding of each physical problem. The governing equations for fluids and solids, and their coupling, form the theoretical foundation for the remainder of this study. Figure 2 summarizes the governing equations for gases, fluids, and elastic solids, along with common coupling models at their interfaces. Specifically, the figure highlights the linear acoustic wave equation in gases, the Navier–Stokes and Cauchy momentum equations in fluids, the conservation of linear momentum, and the linear elastic wave equation in anisotropic solids. Note that the Navier–Stokes and Cauchy momentum equations are applicable in gases when transport and nonlinearities are non-negligible, as is the case in aeroacoustics. More complex elastic wave equations may be necessary to capture motion in elastic microstructured metamaterials containing small-scale asymmetries, such as chirality, to tailor the fluid–solid interaction<sup>1–3</sup>. This set of equations provides a unified framework for analyzing how structured media interact with fluids and acoustic waves. The following sections will illustrate how this framework is applied to specific problems.

In periodic media, such as phononic crystals or acoustic metamaterials, wave propagation is often analyzed using *Bloch's theorem*. This theorem states that the solution to a wave equation in a periodic medium can be written as a Bloch wave—a plane wave modulated by a periodic function. As a result, the analysis can be confined to a single unit cell with Bloch-periodic boundary conditions. Solving the corresponding eigenvalue problem yields the *dispersion relation*, which provides essential information such as the phase and group velocities, as well as potential stop bands or complete band gaps. Fluid flows<sup>4</sup> are

typically characterized by the *Reynolds number*, defined as

$$Re = \frac{\rho_F v L}{\mu_F},$$

where  $\rho_F$  is the fluid density,  $v$  is a characteristic velocity,  $L$  is a characteristic length scale, and  $\mu_F$  is the dynamic viscosity. This dimensionless quantity helps distinguish between different flow regimes: laminar flow dominates at low Reynolds numbers (viscous forces prevail), while turbulent flow emerges at high Reynolds numbers (inertial forces dominate), with a transitional flow regime in between. Knowledge of the flow regime is critical for selecting appropriate models and analysis methods.

The main numerical methods for modeling fluid–structure interactions can be grouped into two broad categories. The methods in the first category, including the finite-element method (FEM), finite-volume method, finite-difference method, the arbitrary Lagrangian–Eulerian method, boundary- and immersed-element methods, solve the Navier–Stokes equations directly<sup>5</sup>. The second category comprises particle-based methods—the lattice Boltzmann method and the smoothed particle hydrodynamics method—that are grounded in the kinetic theory<sup>6</sup>.

In summary, the equations presented in Fig. 2 support the three main sections in this review paper, organized by application domain, and followed by a final “Conclusion and perspectives” section.

### Flow–structure interactions

The ability to engineer the internal structure of materials at the interface with fluids in a manner that enables targeted, desirable interactions opens a broad range of opportunities for controlling fluid flows, thereby potentially improving the responses and overall performance of aero/hydrodynamic systems. Such improvements can manifest as a reduction in drag, an increase in lift, and/or the attenuation of unsteady loads, thereby reducing fatigue. The plurality of flow regimes and available concepts related to architected structures provides us with a wealth of flow–structure interactions. The salient details of such fluid–structure interactions are specific to the particular combination of architected structure and flow regime, as conceptualized in Fig. 3.

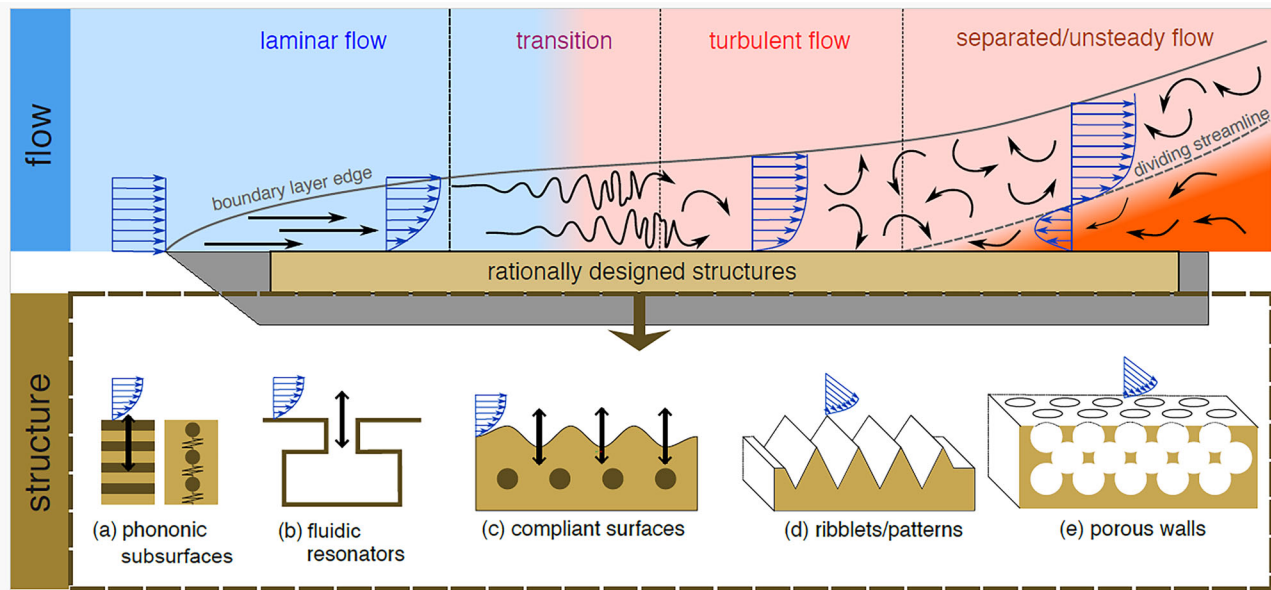


**Fig. 3 | Conceptualization of typical flow regimes interacting with engineered surfaces/subsurfaces.** (Top) Schematic representation of typical flow regimes in order of increasing unsteadiness. (Bottom) Structural solutions for flow control,

**a** Phononic Subsurfaces (PSubs)<sup>9,12,13,18,20,54</sup>, **b** fluidic resonators<sup>19,66,67</sup>, **c** compliant surfaces<sup>21,23,30,31</sup>, **d** riblets<sup>58,224</sup> or patterns<sup>34,35,52,53,61,62,69</sup>, and **e** porous walls<sup>47,65,225</sup>.

### Interactions with transitional flow instabilities

In many types of flows, the transition from the laminar to the turbulent state is primarily driven by the inception, development, and growth of convective flow instabilities, also known as hydrodynamic instabilities<sup>7</sup>. A prominent example in two-dimensional (i.e., non-swept wing) flows are Tollmien–Schlichting (TS) waves. The initially linear behavior of TS wave modes has inspired active control strategies based on the principle of localized perturbation superposition, namely the conscious creation of a “counter response” of the same amplitude yet phase-delayed by 180° with respect to the original TS wave<sup>8</sup>. This can be achieved actively via oscillating surface actuation, creating a response normal to the vertical perturbation component of a propagating wave. In the realm of passive flow control, the concept of phononic subsurfaces (PSubs) emerged over the last decade to generate the desired phased interference in a responsive, functionally effective manner<sup>9</sup>. A PSub relies on the excitation and management of elastic waves within a phononic material<sup>10</sup> buried beneath the surface, nominally forming a single-input, single-output system. These systems are typically constructed from periodic materials (phononic crystals)<sup>9,11,12</sup> or locally resonant materials (elastic metamaterials)<sup>13–15</sup>, effectively forming a precisely engineered subsurface phonon environment interacting with the flow instabilities. The wave dispersion properties of a PSub, as well as its frequency response function as a truncated finite phononic structure<sup>16,17</sup>, can be tailored to generate precise control of the amplitude and phase, thereby stabilizing or destabilizing the TS waves, depending on the target objective. An alternative to phase control, a PSub may be tuned as a phononic diode to extract and trap undesired perturbations in the flow<sup>18</sup>. A present challenge in exciting PSubs using TS waves is the inherently low amplitude of the latter (typically,  $\mathcal{O}(10^{-6} \times U_\infty)$  during linear growth and  $\mathcal{O}(10^{-2} \times U_\infty)$  when transition onsets), which in airflows produce pressure footprints of  $\mathcal{O}(\text{mPa})$ . Such weak forcing results in a large impedance mismatch at the fluid–structure interface, particularly when the fluid is a gas (e.g., air). This may potentially be remedied by tuning the PSub properties to simultaneously exhibit a target compliance over and above the desired phononic properties. The impedance-mismatch obstacle may also be handled using fluidic/acoustic single-input, single-output systems such as Helmholtz

resonators<sup>19</sup>. In both PSubs and Helmholtz resonators, attenuation of TS instabilities has been demonstrated when surface displacement is out-of-phase relative to the local TS wave pressure footprint. This leads to local stabilization in the regions of the control surface. To achieve downstream transition delay, a multi-input, multi-output PSub system has been demonstrated<sup>20</sup>, and recently the notion of a lattice of PSubs was shown to enable downstream stabilization as well<sup>15</sup>.

Looking back from a historical perspective, early fundamental research on the passive mitigation of TS waves via flexible walls was established in the 1960s<sup>21,22</sup> and comprehensively reviewed in the early 2000s<sup>23</sup>. The interaction between the near-wall flow and a compliant wall gives rise to a complex interplay of instabilities, which were first systematically documented and categorized<sup>24</sup>. Local stability analysis showed that the flexibility of a compliant wall tends to stabilize TS waves, whereas the structural viscoelastic effects introduce a slight destabilizing influence<sup>25</sup>. In another study, the fluid–structural interaction between a compliant wall and the boundary layer was found to be destabilizing, as the structural compliance can exacerbate coupled fluid–structural instabilities of Rayleigh–Taylor type<sup>26</sup>. Multilayered compliant wall configurations have been proposed to engender additional control utility on both the elastic compliance and viscous effects<sup>27</sup>. Recently, more advanced global stability analysis methods, such as transient<sup>28</sup> and forced<sup>29</sup> responses, led towards the optimization of local material properties in the compliant wall structure<sup>30</sup>, uncovering streamwise quasi-periodic patterns that are reminiscent of phononic Bragg scattering behavior, paving the way to a concept that has been targeted in a recent study to tackle a TS wave and a flutter instability simultaneously<sup>31</sup>.

The use of structured materials to control flow instabilities was recently shown to extend beyond subsonic TS waves. Periodic surface modifications in the form of shallow cavities have been suggested for stabilizing hypersonic boundary layers<sup>32</sup>, achieving a near-zero impedance condition at the wall, thus effectively suppressing the growth of the dominant viscous instability, namely the second Mack mode. In swept-wing boundary layers, the dominant mechanism of transition is crossflow instabilities, which manifest as stationary, co-rotating vortices roughly aligned with the free-stream flow<sup>33</sup>. Linear superposition and attenuation of stationary crossflow modes were recently achieved

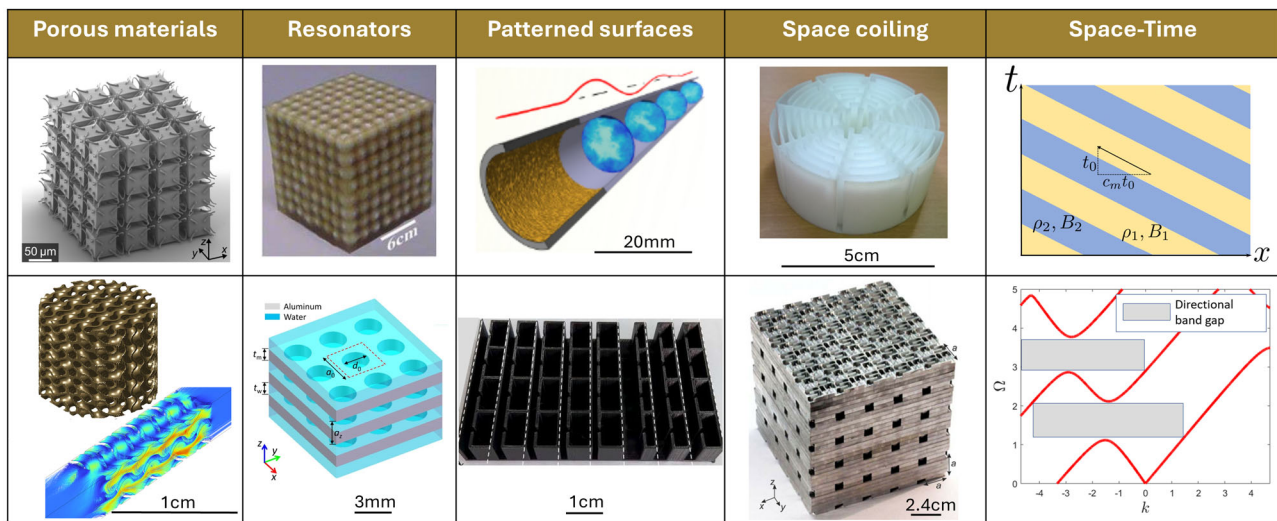


**Fig. 4 | Examples of metamaterials for controlling acoustic waves and flow regimes.** *Poroelastic metamaterials* exhibit effective negative compressibility when subjected to an increase in external air pressure<sup>58</sup>. Porous inserts have been used for decades to reduce internal flow turbulence, while triply-periodic minimal structures deliver more predictable turbulence reduction<sup>53</sup>. *Local resonators*: acoustic metamaterials with local resonators operate in subwavelength regimes by controlling sound waves of wavelengths much larger than their dimensions (top image is from ref. 226). *Patterned surfaces*, including riblets, viscous coatings (top), and periodic inserts, are widely applied to mitigate turbulence in pipes<sup>227</sup>. At the

same time, labyrinthine metasurfaces (bottom) are excellent broadband low-frequency sound absorbers<sup>228</sup>. *Space coiling*: labyrinthine metamaterials characterized by complex internal geometries that manipulate wave propagation through extreme path lengthening<sup>229,230</sup>. *Spatiotemporally-periodic bi-materials* (top): space-time property map with the properties (e.g., the mass density and the bulk modulus) with wave-like periodic dependence on both space and time and modulation speed  $c_m$ . (bottom): asymmetric dispersion diagram presenting directional band gaps in the case of subsonic modulation ( $0 < c_m < \min(c_1, c_2)$ ).

by deploying arrays of periodic roughness elements on the swept-wing surface<sup>34–37</sup>. Such periodic surface architecture can be designed to target specific amplitude, wavelength, and phase characteristics to generate velocity disturbances that interact destructively, thereby attenuating the crossflow instabilities and delaying transition to turbulence.

At low Reynolds numbers, hydrodynamic instabilities emerge as wakes behind solid objects in flowing fluids due to frictional flow resistance. Frictional fluidic force can be reduced by implementing anisotropic mapping of the permeability tensor to realize the control function through a porous structure<sup>38</sup>, active hydrodynamic metamaterials<sup>39</sup>, or passive cloaking<sup>40</sup>.

### Interactions with unsteady and separated flows

Beyond the paradigm of laminar flows exhibiting steady behavior and turbulent flows characterized by chaotic unsteadiness, regimes of (quasi-)deterministic unsteadiness can occur under specific conditions. The emergence of these states is often governed by the interplay between inertial and viscous forces, which is quantified by the Reynolds number. Depending on this ratio, such unsteady regimes may either represent the asymptotic flow behavior or constitute a transitional pathway culminating in turbulence. Typical examples are wakes of bluff bodies, mixing layers and jets, and separated boundary-layer flows. Separated flows often follow geometry-induced or externally imposed increases in pressure (i.e., an adverse pressure gradient), during which the velocity in the boundary layer decelerates and eventually reverses. A direct consequence of flow separation is a significant increase in boundary-layer thickness, leading to a loss of lift and an increase in drag. Furthermore, separated shear layers are inherently unsteady due to their inflectional shape, leading key parameters like velocity, pressure, and temperature to become temporally transient. The ability to postpone or mitigate separation in relevant engineering systems, such as aircraft, ground

transport vehicles, or turbomachinery, can significantly reduce drag, enhance lift, and minimize unsteady structural loads<sup>41</sup>.

Flow control methods to prevent separation typically involve increasing turbulent mixing at the wall near the separation point by passive or active means (e.g., porous coatings or structures (Fig. 4, column ‘Patterned surfaces’), jets, slats or flaps, plasma actuators, acoustic actuators, morphing architectures)<sup>42,43</sup>. Separation can be passively prevented by using distributed vortex generators to induce mixing between upper and lower stratifications within the boundary layer<sup>44</sup>, by contouring a structure to decrease the adverse pressure gradients that lead to separation, or by adding patterned surfaces (e.g., vanes or riblets, Fig. 4, column ‘Patterned surfaces’) to the surface to increase mixing at the separation point. Plasma actuators based on the dielectric barrier discharge mechanism have been used in various external-flow applications, from low to supersonic speeds<sup>45</sup>. Synthetic jets have been used to control flow separation by altering the local pressure and vorticity distributions<sup>46</sup>. Porous coatings have been applied to alter the wake structure and reduce drag on a bluff body<sup>47,48</sup>, and recently there have been efforts on decoupling the effects of porosity and permeability for control over the flow structure and pressure drop around porous structures (Fig. 4, column ‘Porous materials’)<sup>49,50</sup>.

PSubs, discussed in Section ‘Interaction with transitional flow instabilities’, are also applicable to separation control, in which the intervention occurs passively through in-phase interference between the vibratory motion of an elastic surface and flow perturbations, causing destabilization<sup>9,13,14</sup>. Some notable efforts for passive separation control include the introduction of microcavities near the leading edge under a wing. These were found to inhibit the bursting of the laminar separation bubble, thereby delaying the onset of dynamic stall<sup>51</sup>. Kirigami sheets have been proposed, designed to create an array of tilted surface elements, which could suppress a separation bubble<sup>52</sup>. Inherent flow unsteadiness, with or without separation, can be unavoidable in certain scenarios. In such cases, the primary objective shifts

to mitigating oscillation amplitudes in the flow, thereby attenuating the periodic loads imposed on the primary structure. Recent investigations have explored the potential of architected materials as effective control devices for such applications. In particular, they have been used to attenuate downstream unsteadiness induced by backward-facing steps<sup>53</sup>, and to stabilize oscillations arising from shock-wave interactions with boundary layers<sup>54</sup>.

### Interactions with turbulent flows

While the previous two sections addressed long-standing and recent developments in the control of transitional and separated flows, the taming of turbulent boundary layers has received its extensive share of foundational and applied research over the past several decades<sup>55–57</sup>. Despite extensive efforts to promote laminar flow, the high Reynolds number occurring in many engineering systems (e.g., aircraft, gas/oil pipes, and turbomachinery) entails a strong dominance of turbulent boundary layers, which exhibit large momentum diffusivity, consequently increasing skin-friction drag and convective heat transfer over surfaces<sup>58</sup>. Upstream turbulent fluctuations are also a known driver of hypersonic shock waves, leading to the onset of severe thermoacoustic loads that can be detrimental to vehicle integrity as well as sources of acoustic noise. Efforts towards controlling turbulent flows have ranged from passive to active approaches, both seeking to destructively interfere with the self-regenerating energy production process driven by sweeps and ejections within a disordered turbulence sequence<sup>59</sup>. In a turbulent boundary layer, most of the energy production occurs very close to the wall, and as a result, most control efforts have revolved around surface texture modifications or altering the fluid properties in the vicinity of the wall. For example, wall riblets and grooves represent one of the earliest and most commonly studied techniques, showing at times skin-friction-drag reduction of up to 10%<sup>58</sup>. Other passive efforts have included superhydrophobic surfaces and polymer drag reducers<sup>60</sup>, systems of micro-canopies<sup>61</sup>, concepts of compliant tensegrity fabrics<sup>62</sup>, and tribological metasurfaces<sup>63</sup>. Similarly, active mechanisms, such as streamwise-aligned plasma actuators for direct drag reduction through Stokes-layer formation, have been proposed<sup>64</sup>.

The notion of utilizing structured materials that invoke concepts of permeability, resonance, and, potentially, wave dispersion has recently gained attention due to rapid advancements in heterogeneous material fabrication technology, especially those with tunable and graded properties. In this space, wall surfaces with anisotropic porosity, engineered perforations, microcavities, fluidic resonators, baffles, and streamwise slots with a common plenum have all demonstrated promising results<sup>65–67</sup>. Wave engineering principles, such as PSubs, have been recently investigated for the purpose of attenuating turbulent-induced unsteadiness in high-speed flows<sup>54</sup>. Other studies have examined the impact of wall-normal blowing and suction on turbulent drag in channel flows, simulating subsurface velocities and setting up the problem for subsurface phononic crystals that respond to wall-normal fluid forces<sup>68</sup>. Alternatively, since the shear force in a wall-bounded flow is directly related to viscosity, wall heating (liquids) or cooling (gases) provides a different path to tackle the same challenge. Motivated by this aspect, wall-aligned heat strips in compressible turbulent channel flows have recently been shown to achieve a notable drag reduction<sup>69</sup>. In this approach, “targeted” control, i.e., the intentional targeting of coherent vortical structures to inhibit turbulence production, necessitates a selective spatial arrangement of streamwise heating strips.

### Surface gravity waves

Another problem related to engineered interaction with fluid flows is the propagation of surface gravity waves, e.g., water waves, in the presence of solid obstacles or structured boundaries<sup>70</sup>. For linear (small-amplitude) gravity waves, the fluid particle motion is

elliptical (circular in deep water, flattened in shallow water), and the particle velocity decays exponentially with depth. Various effects have been demonstrated in this setting, including wave focusing<sup>71</sup>, cloaking<sup>72</sup>, superscattering<sup>73</sup>, and wave guiding<sup>74</sup>. The main strategies adopted so far to manipulate water waves rely on periodically distributed submerged or surface-emerging pillars or periodical depth variations, i.e., variable bathymetry. For example, band gaps for water waves have been obtained using periodic arrays of immersed resonators such as vertical tubes, an effect that the authors compare to a “negative gravitational acceleration”<sup>75,76</sup>. Metasurfaces have been effectively used to generate band gaps, for example, using a periodically drilled bottom<sup>77</sup>, or activating Bragg scattering by arrays of floating plates and/or submerged trenches<sup>78</sup>. Numerical models have been adopted to describe the interaction of periodic structures with water waves, predicting refraction<sup>79</sup>, scattering<sup>78</sup>, or rainbow effects in spatially graded arrays<sup>80,81</sup>. Other experimental studies have demonstrated reflectionless waveguiding in curved channels realized with a layered metamaterial structure<sup>82</sup>. On the other hand, relatively few studies have considered the possibility of employing periodic arrangements of submerged resonators to control water waves, partially due to the complexity of the problem involving resonator oscillations coupled with their motion in a fluid, with correlated surface and viscous effects. Recently, the concept of an inverted subsurface pendula has been introduced to couple both local resonance and Bragg effects and generate band gaps in water waves<sup>83,84</sup>.

### Flow-induced acoustic interactions with metamaterials

In many practical applications (e.g., in aerospace, energy, and turbomachinery systems) involving acoustic metamaterials, the presence of background flows cannot be neglected. The interaction of acoustic waves with both the surrounding structures and flow determines how sound is generated, transmitted, or suppressed. This section focuses on two main categories relevant to acoustics and flow: noise generation and mitigation in the presence of grazing flow (Section “Metamaterials interacting with grazing flows and/or acoustic waves”), and particle manipulation in fluids (Section “Particle manipulation by acoustic field”).

#### Metamaterials interacting with grazing flows and/or acoustic waves

In aeronautics, acoustic metamaterials have been proposed as noise-control technologies to reduce surface pressure fluctuations and suppress aeroacoustic sources<sup>85</sup>. Applications include trailing-edge noise mitigation in wind turbines<sup>86–88</sup>, noise due to turbulence-surface interaction in engines and propellers<sup>89–91</sup>, and landing-gear noise reduction<sup>92</sup>. Other fields of application, in which metamaterials are often named as ventilated metamaterials<sup>93–95</sup>, are noise control in heating, ventilation, and air conditioning systems for residential and office spaces, and sound generation of high-speed flows in piping of industrial equipment<sup>96</sup>. All these applications share the presence of a grazing flow.

Flow-permeable surfaces are common solutions when the control strategy aims to reduce the amplitude of the surface pressure fluctuations via a pressure balance mechanism<sup>97,98</sup>. However, their capability to mitigate noise depends on parameters such as permeability and pressure-balance coefficients, which vary significantly under grazing flow conditions where convection dominates<sup>99–101</sup>. To assess the impact of the two coefficients separately and decouple the effect of the geometry on both the aerodynamic and acoustic field, triply periodic minimal surfaces are often used<sup>102</sup>. These interactions between flow and metamaterial structures (which are usually rough surfaces) generate vorticity and alter turbulence, thereby complicating both prediction and design of improved acoustic surfaces<sup>103</sup> and can affect the aerodynamic performances.

On the other hand, if the goal is to reduce the amplitude of the acoustic waves generated by the fluid field, traditional solutions to these problems, such as local resonators (Fig. 4, column ‘Resonators’), branch Helmholtz or quarter-wavelength resonators, expansion and plenum chambers, mufflers<sup>104</sup>, and Herschel–Quincke tubes<sup>105</sup>, space-coiling designs (Fig. 4, column ‘Space coiling’) and similar branching structures<sup>106,107</sup> provide narrow-band noise isolation with minimal disruption to fluid flow. These architected acoustic wave filters predate metamaterial solutions by many decades and may, in fact, be viewed as precursors to recent metamaterial research. Broadband acoustic absorbers in current industrial applications primarily consist of acoustic liners constructed from porous media or micro-perforated structures, both of which provide reduced acoustic isolation when compared to resonant structures and can restrict flow<sup>104,108,109</sup>.

Ventilated acoustic metamaterials represent a merging of new scientific concepts and fabrication capabilities with classical solutions to acoustical problems, addressing longstanding noise-control challenges<sup>96,110</sup>. These solutions are generally constructed using two components: (i) one region that allows the flow of gas or fluid and (ii) another that contains subwavelength geometries to generate high acoustic isolation via resonance<sup>110</sup>. They can be made geometrically compact by leveraging space-coiling designs<sup>111</sup> with various form factors, including labyrinthine<sup>112–115</sup> and helical<sup>116–119</sup> architectures arranged at duct boundaries or at interfaces between domains through which fluid flow is desired. This approach has been generalized to create structures that surround acoustic sources in free space, providing acoustic isolation while allowing flow through the volume<sup>120,121</sup>. The key attribute of ventilated acoustic metamaterials is the ability to design performance in an acoustically compact space, enabling tailored acoustic isolation for target broadband<sup>114,117,122–124</sup> and even tunable<sup>125,126</sup> isolation. Ventilated acoustic metamaterials, therefore, represent a highly promising and practical solution for applications where flow is an essential feature of system functionality and noise control is required.

To investigate these concepts, many research groups have developed dedicated test rigs that include fluid flows<sup>127–131</sup>. It has been found that the interaction between the acoustic field, the metamaterial and the fluid flow depends on several parameters such as the sound pressure level, the boundary layer properties and the surface topology<sup>132</sup>. The drag penalty associated with metamaterials has also become a central concern, which must be a key consideration for metamaterial solutions. Experiments have confirmed that coatings with perforated resistive layers can increase viscous drag under strong acoustic excitation, underscoring the need to balance acoustic benefits with aerodynamic penalties<sup>133,134</sup>.

### Particle manipulation by an acoustic field

Controlled manipulation of particles at the microscale and nanoscale is essential across a wide range of scientific and technological fields, from particle physics to biomedicine. It plays a critical role in studying biological processes at the single-cell or subcellular vesicle level, identifying protein biomarkers associated with specific diseases, assembling DNA, and understanding fundamental particle dynamics<sup>135</sup>. Microfluidic technologies have emerged as powerful tools for particle manipulation, enabling transportation, separation, trapping, and enrichment through various mechanisms, including hydrodynamic, acoustic, electrical, optical, and magnetic methods. However, due to the extremely small size of nanoparticles, direct mechanical manipulation is often impractical. As a result, non-contact methods—typically involving dynamic control of external gradient force fields—are preferred. Among different methods, acoustofluidics<sup>136</sup>—the use of sound waves to exert forces within fluidic environments—has gained significant attention. This approach is particularly attractive due to its non-contact, label-free nature, high biocompatibility, and the ability to manipulate particles over relatively large volumes. These systems

commonly employ surface acoustic waves<sup>137,138</sup> or bulk acoustic waves<sup>139</sup>, which are typically employed to achieve precise control over particles in acoustic tweezers<sup>140</sup>. Acoustofluidic devices manipulate fluids and particles using acoustic radiation forces and streaming (Fig. 4, column ‘Resonators’). When a traveling surface acoustic wave encounters a liquid, its higher viscosity causes part of the wave to refract as a longitudinal wave, forming a ‘leaky’ or ‘pseudo’ surface or bulk acoustic wave. Reflections at the liquid boundaries induce acoustic streaming—a nonlinear effect that converts wave attenuation into steady fluid flow, enabling manipulation of suspended particles<sup>137</sup>. Although acoustic radiation forces enable precise control, their strength is inversely proportional to both the fluidic channel dimensions and the acoustic wavelength<sup>141</sup>. Consequently, achieving high-resolution manipulation at the micrometer scale typically requires high-frequency interdigital transducers and complex electronic systems, which are costly and technically demanding. Recent advances in additive manufacturing offer novel solutions to these limitations<sup>142</sup>, allowing the fabrication of corrugated surfaces and phononic crystals for advanced particle manipulation<sup>143,144</sup>.

In particular, acoustofluidic metasurfaces composed of sub-wavelength arrangements of inclusions, pillars, or other rationally designed composites show strong potential for fluid manipulation, particle trapping and spectrally and spatially selective droplet motion control at scales well below the acoustic wavelength in the plain medium<sup>145–147</sup>. Parallel to this, the controlled manipulation of particles by acoustic radiation forces enables the tuning of the acoustic properties of colloidal assemblies, leading to three-dimensional colloidal phononic crystals that are reconfigurable in real time and capable of rapidly altering their frequency-filtering characteristics<sup>148</sup>. Note that combining diverse metasurface geometries and tailored particle suspensions will enable the generation of even more complex acoustic fields and fluid flows without relying on intricate arrangements of interdigital transducers.

### Exotic metamaterial concepts in fluid-structure interaction

Elastic metamaterials provide a powerful platform for controlling fluid–structure interaction by coupling structural vibrations with pressure waves in gases and liquids. Their engineered architecture allows the creation of band gaps, local resonances, and anisotropic responses that may potentially help suppress turbulence, reduce drag, and dampen flow-induced vibrations. Classical elastic materials are modeled by Cauchy elasticity, where matter is treated as being composed of infinitesimally small volume elements that can be described by purely translational displacements. This approximation holds when atomic dimensions are negligible compared to vibration wavelengths. In contrast, metamaterials can have much larger unit cells, enabling vibrational resonances at relevant frequencies<sup>149</sup> and Bragg scattering with phononic band gaps<sup>150</sup>. Unit cell deformations introduce behavior beyond Cauchy elasticity<sup>3</sup>, requiring generalized frameworks such as micropolar elasticity<sup>151</sup>. Long-range coupling between unit cells can induce nonlocal effects<sup>152</sup>, and modulating material properties in both space and time enables symmetry-breaking and non-reciprocal behavior<sup>153–155</sup>. Most mechanical metamaterials comprise solid matrices with internal voids often assumed to be vacuum. In reality, these voids are filled with air or water, allowing weak but significant coupling between solid elastic and fluid pressure waves<sup>156</sup>. This interaction, though often neglected due to impedance mismatch, creates opportunities for wave control. In airborne or waterborne media, rigid-wall assumptions<sup>157</sup> dominate, but poroelastic metamaterials (Fig. 4, column ‘Porous materials’) demonstrate active fluid–structure coupling<sup>158,159</sup>. The following subsections explore how topological, nonlocal, and time-varying metamaterials may be used to enhance wave control in flow environments.

## Topological interactions

Acoustic and elastic topological systems<sup>160,161</sup>, like their electromagnetic counterparts<sup>162</sup>, exhibit bulk-edge correspondence, where the periodic band structure determines the presence of robust edge or surface modes, insensitive to certain types of defects and disorder, and immune to backscattering<sup>163–165</sup>. Underpinning the topological nature of the Bloch bands are associated invariants, which characterize the geometric phase, that is, the phase change associated with a continuous adiabatic deformation of the system; most notably, the Berry phase<sup>166</sup> and its one-dimensional counterpart, the Zak phase<sup>167</sup>. Many topological insulators have been translated into wave physics using Lieb, kagome lattice<sup>168</sup>, or glide-reflection symmetric crystal interfaces<sup>169</sup>. These points enable the formation of edge states at interfaces between topologically distinct media and have been adapted for waveguiding, localization, and sensing<sup>170</sup>. More recently, interest has shifted to so-called higher-order topological insulators and semimetals, a novel class of structures where topologically protected modes emerge at lower-dimensional boundaries such as corners or hinges, enabling robust control of sound and mechanical waves beyond conventional topological phases<sup>171,172</sup>. These materials are said to generalize the conventional bulk-boundary correspondence, recognizing that nontrivial bulk topology can manifest not only at edges but at lower-dimensional features<sup>173,174</sup>. Many experimental demonstrations of topological phononic systems have used acoustic waves propagating in the air, mostly neglecting the interaction with the solid skeleton that surrounds the wave system<sup>175–178</sup>. Topological edge states have also been considered in water wave systems that support highly dispersive wave propagation, in the gravity capillary wave regime<sup>179,180</sup>. In the case of crystal structures composed of steel inclusions immersed in water, it was found that fluid-structure interaction must be taken into account to faithfully describe the propagation of acoustic waves, and especially the frequency position of Dirac points<sup>181</sup>. To date, topological wave systems have thus primarily been explored in single-phase media (solid or fluid), with limited understanding of the complex interactions that can occur between a vibrating structure and fluid dynamics. One notable exception is the demonstration of a novel approach to topological phononics by exploiting the interplay between fluid-borne and solid-borne sound waves, leading to the experimental realization of type-II nodal rings in a simple three-dimensional phononic crystal<sup>182</sup>. Through combined theoretical and experimental analysis, the authors reveal that fluid–solid interactions enable strongly tilted drumhead surface states, offering a robust and easily implementable platform to explore advanced topological phenomena in flow-coupled systems. Another recent demonstration of on-chip topological acoustofluidics reveals the complex interplay between phonon valleys, nonlinear fluid dynamics, and the crystallographic structure of the substrate within a microfluidic environment<sup>183</sup>. The study reports the formation of topological pressure nanowells that enable DNA molecule concentration via confined edge modes, offering a new approach to probing biological behavior in fluid and solid media. It also highlights the orientation dependence of acoustofluidic edge states on substrate crystallography. In addition, flat bands with zero-group velocity have recently shown the potential to localize energy at higher amplitudes, which offers an exciting avenue for engineering space–time response or phase in flow dynamics<sup>184</sup>. These findings are expected to open new avenues for the integration of topological materials with various applications and the exploration of topological phenomena in complex media.

## Local and nonlocal interactions

The Cauchy elasticity equations shown in the green part of Fig. 2 are local: stress at one point produces strain only at that point<sup>185</sup>. This assumption relies on modeling materials by infinitesimally small volume elements, which breaks down in metamaterials with finite-

sized unit cells. In contrast, *nonlocal elasticity* allows the strain at one point to depend on stresses elsewhere, modeled through spatial dispersion in reciprocal space or convolution in real space<sup>186</sup>. Nonlocal effects in metamaterials arise from higher-order interactions, soft modes, chirality, or time-dependent couplings, as reviewed elsewhere<sup>154</sup>. In the static regime, they are linked to decaying Bloch modes or “frozen evanescent phonons”<sup>187,188</sup>, whose long decay lengths produce size effects that can exceed tens of unit cells. Under specific boundary conditions, such structures can exhibit responses that deviate significantly from the assumptions of classical elasticity. Interestingly, static nonlocal elasticity maps mathematically to Ohm’s law in incompressible electron fluids and laminar fluid flow in networks via Hagen–Poiseuille’s law. This analogy has revealed the emergence of backward currents—flows that oppose the primary direction due to oscillating solutions of the Bloch problem<sup>189</sup>. These induce laminar-scale vortices, mimicking effects normally associated with turbulence, and may offer new pathways for fluid manipulation in metamaterial-based channels. In dynamics, nonlocal metamaterials can produce roton-like dispersion with backward-propagating phonons<sup>190</sup>, enabling precise wave shaping. Through Fourier synthesis, arbitrary dispersion relations can be engineered by tuning beyond-nearest-neighbor interactions<sup>191,192</sup>. Poroelastic metamaterials, which incorporate fluid-filled voids in elastic matrices, are especially relevant here. They enable strong coupling between pressure waves and solid deformation, unlike rigid-wall assumptions<sup>158,159</sup>.

## Space–time metamaterials

Space–time metamaterials or spatiotemporally modulated metamaterials are a class of metamaterials, the properties of which are modulated not only in space but also dynamically in time, enabling unprecedented control over wave propagation. This combined space–time modulation breaks reciprocity and gives rise to a range of exotic wave phenomena. These include non-reciprocal wave propagation, where waves can travel in one direction but are blocked in the opposite one, asymmetric transmission, unidirectional amplification, and frequency and wavenumber conversion. Notably, spatiotemporal modulation enables these phenomena without the need for magnetic-field biasing or material nonlinearity. Such properties have opened new frontiers in designing devices for wave manipulation in acoustics<sup>193</sup>, elastodynamics<sup>155,194</sup>, electromagnetics<sup>195</sup>, surface Rayleigh waves<sup>196</sup>, diffusion<sup>197,198</sup>, flexural waves<sup>199</sup>, flexural-gravity waves<sup>200</sup>, water waves<sup>201</sup>, with potential applications in isolation, sensing, communication, and vibration control. Many works have focused on the case of wave-like space–time modulations of the physical properties<sup>202–204</sup> as indicated in the space–time property map shown in Fig. 4, column “Space–time”. Effective-medium models have been derived for this case, yielding non-reciprocal Willis coupling, or bianisotropic models, if both the density and modulus are modulated in phase<sup>205–207</sup>. As a result, waves propagating in space–time modulated media break the  $k \leftrightarrow -k$  symmetry. In parallel, other studies have explored the role of time-modulated boundary conditions<sup>208</sup>, time-modulated interfaces<sup>209</sup>, or time-modulated resonators embedded in a quiescent background medium<sup>210,211</sup> to achieve similar symmetry-breaking effects. Additional uses of space–time modulation at domain boundaries or interfaces between domains include non-reciprocal scattering, pseudo-Doppler effects, and space–time encoding of scattered fields as previously studied in the context of electromagnetic metasurfaces<sup>212</sup>.

Another perspective on metamaterials concerns exotic wave manipulation achieved through unconventional constitutive relations, in which the link between stress and the external field can be tailored to realize a desired acoustic mirage<sup>213</sup>. This extended continuum model, referred to as a metacontinuum, can be coupled with the space–time relativistic reformulation of the governing equations<sup>214,215</sup>. In this formulation, the non-uniform background flow plays the same role that the mass has in general relativity, inducing a local intrinsic

curvature of the space-time (see, e.g., ref. 216). According to this analogy, the intrinsic geometry of the acoustic space-time can be a precious tool for an alternative interpretation of the aerodynamic convection. Following this approach, the governing equations are form-invariant, enabling straightforward application of space–time transformations to directly embed the characteristics of the flow into the metacontinuum design<sup>101</sup>. This allows for an easy correction of a metacontinuum conceived to operate in a quiescent medium, to take into account a background aerodynamic flow. This approach strengthens the theoretical understanding of wave-propagation phenomena and supports the development of advanced aeroacoustic devices based on exotic continua. The performance and the limitations of this approach have been extensively assessed through accurate numerical simulations<sup>217,218</sup>, making it sufficiently mature to be coupled to inverse-design methodologies and optimization strategies.

At present, very few works combine the concept of space–time metamaterials and fluid flows, although it is notable that there is a well-established community using active control and feedback to delay the transition to turbulence, lower drag and wing loads, and optimize aerodynamic performance<sup>219,220</sup>. Nevertheless, introducing time variation into material properties and boundary conditions seems to be the key to amplifying the range of exotic wave manipulations. On one hand, the physical symmetries breaking obtained with space-time modulated materials are beginning to be applied to flow control, e.g., using active subsurface acoustic diodes to extract undesirable flow perturbations<sup>18</sup>. On the other hand, recent works provide a methodology for deriving space–time-corrected metacontinua able to preserve the efficiency in convective environments by including the external aerodynamic flow directly into the device design. The combination of these two approaches could pave the way for the development of an adaptive modulation strategy to enhance the flow capabilities of the device.

## Discussion and outlook

This review discusses the rich and multifaceted field of coupling between material architectures and fluid flows, highlighting a range of distinctive metamaterial and wave manipulation principles and emphasizing recent advances in theory, experiment, and applications. It examines how structured materials engineered at micro- to macroscales can modulate, suppress, or amplify flow-related phenomena such as boundary- or shear-layer instabilities, surface acoustic emissions, and flow-induced structural vibrations. Across laminar, transitional, and turbulent regimes, phonon engineering of flow-bounded walls is showing great promise for controlling boundary-layer development, delaying separation, and minimizing drag. In acoustics, flow-permeable materials and aeroacoustic liners are being successfully adapted to reduce broadband noise and manage convective effects in complex environments. Emerging elastic metamaterial concepts are enabling localized vibration control and energy trapping, particularly through resonant and topological mechanisms. The incorporation of engineered elastodynamic, porous, and patterned interfaces has begun to shift the paradigm of flow control from empirical surface treatments to physics-informed design of functional surfaces and subsurfaces.

What distinguishes metamaterials and phononic material engineering concepts from conventional materials in this context is the capacity to enable wave-based control strategies—leveraging dispersion, periodicity, local resonance, impedance mismatch, and anisotropy to manage fluid–solid coupling and flow instabilities at a fundamental level. Through approaches such as phononic subsurfaces, diodic structures, and compliant phononic-crystal coatings, researchers have demonstrated unique passive and semi-active methods for managing flow behavior in various systems, including channels, aerofoils, inlets, cavities, and underwater bodies. Although

integration into large-scale applications remains challenging, the theoretical foundation and proof-of-concept results offer a compelling path forward.

Looking ahead, integration of cutting-edge metamaterial principles promises to unlock powerful new fluid–structure interaction capabilities. Expanding the use of nonlocal, anisotropic, and topological effects may enable control beyond the current classes of surface interactions, targeting complex disturbance propagation within fluid or structural domains—including in high-Reynolds-number flows. Programmable and reconfigurable metamaterials hold promise for creating flow-responsive systems that adapt in real time to changing conditions, enabling active control of boundary layers, flow separation, and acoustic noise. In addition, multiphase and poroelastic materials with graded impedance or compliance at the fluid–solid interface could enable smoother, more efficient control strategies. Incorporating time-varying material properties may break reciprocity limits and harness flow instabilities for energy extraction. To avoid degradation issues associated with compliant metamaterials, topological mechanical metamaterials—such as Maxwell lattices<sup>221–223</sup>—could be explored for their versatile rigidity characteristics.

Realizing these opportunities will require tightly integrated modeling, fabrication, experimentation, and, critically, close collaboration between the fluids and structural dynamics communities. A future prospect is to move beyond passive structures toward metamaterials that actively shape fluid behavior with machine learning—enhancing performance and efficiency in aerospace, marine, energy, biomedical applications, and other systems.

## References

1. Milton, G. W. & Willis, J. R. On modifications of Newton's second law and linear continuum elastodynamics. *Proc. R. Soc. A* **463**, 855–880 (2007).
2. Maugin, G. A. & Metrikine, A. V. *Mechanics of Generalized Continua. Advances in Mechanics and Mathematics* (Springer, US, 2010).
3. Frenzel, T., Kadic, M. & Wegener, M. Three-dimensional mechanical metamaterials with a twist. *Science* **358**, 1072–1074 (2017).
4. Tritton, D. J. *Physical Fluid Dynamics* (Springer Science & Business Media, 2012).
5. Lomax, H., Pulliam, T. H., Zingg, D. W., Pulliam, T. H. & Zingg, D. W. *Fundamentals of Computational Fluid Dynamics*, vol. 246 (Springer, 2001).
6. Bazilevs, Y., Takizawa, K. & Tezduyar, T. E. *Computational Fluid-structure Interaction: Methods and Applications* (John Wiley & Sons, 2013).
7. Kachanov, Y. S. Physical mechanisms of laminar-boundary-layer transition. *Annu. Rev. Fluid Mech.* **26**, 411–482 (1994).
8. Milling, R. W. Tollmien–Schlichting wave cancellation. *Phys. Fluids* **24**, 979–981 (1981).
9. Hussein, M. I., Biringen, S., Bilal, O. R. & Kucala, A. Flow stabilization by subsurface phonons. *Proc. R. Soc. A* **471**, 20140928 (2015).
10. Hussein, M. I., Leamy, M. J. & Ruzzene, M. Dynamics of phononic materials and structures: historical origins, recent progress, and future outlook. *Appl. Mech. Rev.* **66**, 040802 (2014).
11. Barnes, C. J., Willey, C. L., Rosenberg, K., Medina, A. & Juhl, A. T. Initial computational investigation toward passive transition delay using a phononic subsurface. In *AIAA Scitech 2021 Forum*, 1454 (2021).
12. Michelis, T., Putranto, A. & Kotsonis, M. Attenuation of Tollmien–Schlichting waves using resonating surface-embedded phononic crystals. *Phys. Fluids* **35**, 044101 (2023).
13. Kianfar, A. & Hussein, M. I. Phononic-subsurface flow stabilization by subwavelength locally resonant metamaterials. *N. J. Phys.* **25**, 053021 (2023).

14. Kianfar, A. & Hussein, M. I. Local flow control by phononic sub-surfaces over extended spatial domains. *J. Appl. Phys.* **134**, 094701 (2023).
15. Hussein, M. I., Roca, D., Harris, A. R. & Kianfar, A. Scatterless interferences: delay of laminar-to-turbulent flow transition by a lattice of subsurface phonons. *Proc. R. Soc. A* (in press).
16. Al Ba'ba'a, H. B., Willey, C. L., Chen, V. W., Juhl, A. T. & Nouh, M. Theory of truncation resonances in continuum rod-based phononic crystals with generally asymmetric unit cells. *Adv. Theory Simul.* **6**, 2200700 (2023).
17. Rosa, M. I., Davis, B. L., Liu, L., Ruzzene, M. & Hussein, M. I. Material vs. structure: topological origins of band-gap truncation resonances in periodic structures. *Phys. Rev. Mater.* **7**, 124201 (2023).
18. Schmidt, R., Yousef, H., Roy, I., Scalo, C. & Nouh, M. Perturbation energy extraction from a fluid via a subsurface acoustic diode with sustained downstream attenuation. *J. Appl. Phys.* **137**, 054901 (2025).
19. Michelis, T., de Koning, C. & Kotsonis, M. On the interaction of Tollmien-Schlichting waves with a wall-embedded Helmholtz resonator. *Phys. Fluids* **35**, 034104 (2023).
20. Willey, C. L. et al. Multi-input multi-output phononic subsurfaces for passive boundary layer transition delay. *J. Fluids Struct.* **121**, 103936 (2023).
21. Benjamin, T. B. Effects of a flexible boundary on hydrodynamic stability. *J. Fluid Mech.* **9**, 513–532 (1960).
22. Landahl, M. T. On the stability of a laminar incompressible boundary layer over a flexible surface. *J. Fluid Mech.* **13**, 609–632 (1962).
23. Carpenter, P. W., Lucey, A. D. & Davies, C. Progress on the use of compliant walls for laminar-flow control. *J. Aircr.* **38**, 504–512 (2001).
24. Benjamin, T. B. The threefold classification of unstable disturbances in flexible surfaces bounding inviscid flows. *J. Fluid Mech.* **16**, 436–450 (1963).
25. Carpenter, P. W. & Garrad, A. D. The hydrodynamic stability of flow over Kramer-type compliant surfaces. Part 1. Tollmien-Schlichting instabilities. *J. Fluid Mech.* **155**, 465–510 (1985).
26. Carpenter, P. W. & Garrad, A. D. The hydrodynamic stability of flow over Kramer-type compliant surfaces. Part 2. Flow-induced surface instabilities. *J. Fluid Mech.* **170**, 199–232 (1986).
27. Yeo, K. S. The stability of boundary-layer flow over single-and multi-layer viscoelastic walls. *J. Fluid Mech.* **196**, 359–408 (1988).
28. Tsigklifis, K. & Lucey, A. D. The interaction of Blasius boundary-layer flow with a compliant panel: global, local and transient analyses. *J. Fluid Mech.* **827**, 155–193 (2017).
29. Pfister, J.-L., Fabbiane, N. & Marquet, O. Global stability and resolvent analyses of laminar boundary-layer flow interacting with visco-elastic patches. *J. Fluid Mech.* **937**, A1 (2022).
30. Pfister, J.-L. *Instabilities and Optimization of Elastic Structures Interacting with Laminar Flows*. Ph.D. thesis (Université Paris-Saclay, France, 2019).
31. Fabbiane, N., Marquet, O., Pierpaoli, L., Cottreau, R. & Couliou, M. Phononic compliant surfaces for the suppression of travelling wave flutter instabilities in boundary-layer flows. *J. Fluid Mech.* **1020**, A47 (2025).
32. Zhao, R., Liu, T., Wen, C. -y, Zhu, J. & Cheng, L. Impedance-near-zero acoustic metasurface for hypersonic boundary-layer flow stabilization. *Phys. Rev. Appl.* **11**, 044015 (2019).
33. Saric, W. S., Reed, H. L. & White, E. B. Stability and transition of three-dimensional boundary layers. *Annu. Rev. Fluid Mech.* **35**, 413–440 (2003).
34. Zoppini, G., Michelis, T., Ragni, D. & Kotsonis, M. Cancellation of crossflow instabilities through multiple discrete roughness elements forcing. *Phys. Rev. Fluids* **7**, 123902 (2022).
35. Zoppini, G. *Receptivity of Swept Wing Boundary Layers to Surface Roughness: Diagnostics and extension to flow control*. Ph.D. thesis, Delft University of Technology (2023).
36. Ivanov, A. & Mischenko, D. Delay of laminar-turbulent transition on swept-wing with help of sweeping surface relief. In *AIP Conference Proceedings*, vol. 2125 (AIP Publishing, 2019).
37. Ustinov, M. & Ivanov, A. Cross-flow dominated transition control by surface micro-relief. In *AIP Conference Proceedings*, vol. 2027 (AIP Publishing, 2018).
38. Urzhumov, Y. A. & Smith, D. R. Fluid flow control with transformation media. *Phys. Rev. Lett.* **107**, 074501 (2011).
39. Urzhumov, Y. A. & Smith, D. R. Flow stabilization with active hydrodynamic cloaks. *Phys. Rev. E-Stat. Nonlinear Soft Matter Phys.* **86**, 056313 (2012).
40. Park, J., Youn, J. R. & Song, Y. S. Hydrodynamic metamaterial cloak for drag-free flow. *Phys. Rev. Lett.* **123**, 074502 (2019).
41. Gad-el Hak, M. & Bushnell, D. M. Separation control. *J. Fluids Eng.* **113**, 5–30 (1991).
42. Ashill, P., Fulker, J. & Hackett, K. A review of recent developments in flow control. *Aeronautical J.* **109**, 205–232 (2005).
43. Cattafesta, L. N. & Sheplak, M. Actuators for active flow control. *Annu. Rev. Fluid Mech.* <https://doi.org/10.1146/annurev-fluid-122109-160634> (2011).
44. Lin, J. C. Review of research on low-profile vortex generators to control boundary-layer separation. *Prog. Aerosp. Sci.* **38**, 389–420 (2002).
45. Corke, T. C., Enloe, C. L. & Wilkinson, S. P. Dielectric barrier discharge plasma actuators for flow control. *Annu. Rev. Fluid Mech.* <https://doi.org/10.1146/annurev-fluid-121108-145550> (2010).
46. Glezer, A. & Amitay, M. Synthetic jets. *Annu. Rev. Fluid Mech.* <https://doi.org/10.1146/annurev.fluid.34.090501.094913> (2002).
47. Klausmann, K. & Ruck, B. Drag reduction of circular cylinders by porous coating on the leeward side. *J. Fluid Mech.* <https://doi.org/10.1017/jfm.2016.757> (2017).
48. Terwagne, D., Brojan, M. & Reis, P. M. Smart morphable surfaces for aerodynamic drag control. *Adv. Mater.* **26**, 6608–6611 (2014).
49. Seol, C., Hong, J. & Kim, T. Flow around porous square cylinders with a periodic and scalable structure. *Exp. Thermal Fluid Sci.* <https://doi.org/10.1016/j.expthermflusci.2023.110864> (2023).
50. Seol, C., Kim, T. & Kim, T. The effect of permeability on the flow structure of porous square cylinders. *J. Fluid Mech.* <https://doi.org/10.1017/jfm.2024.311> (2024).
51. Visbal, M. R. & Garmann, D. J. Passive control of dynamic stall using a flow-driven micro-cavity actuator. *Theor. Comput. Fluid Dyn.* **37**, 289–303 (2023).
52. Wen, X. et al. Dynamic kirigami structures for wake flow control behind a circular cylinder. *Phys. Fluids* **35**, 011707 (2023).
53. Piest, B., Druetta, P. & Krushynska, A. Mitigation of flow-induced vibrations in high-speed flows using triply periodic minimal surface structures. *Phys. Fluids* **36**, 105119 (2024).
54. Navarro, J. D. et al. Stabilization of hypersonic shockwave/boundary-layer interactions with phononic metamaterials. *Matter* **8**, 102089 (2025).
55. Gad-el Hak, M. Modern developments in flow control. *Appl. Mech. Rev.* **49**, 365–379 (1996).
56. Abbas, A. et al. Drag reduction via turbulent boundary layer flow control. *Sci. China Technol. Sci.* **60**, 1281–1290 (2017).
57. Corke, T. C. & Thomas, F. O. Active and passive turbulent boundary-layer drag reduction. *AIAA J.* **56**, 3835–3847 (2018).
58. Ghaemi, S. Passive and active control of turbulent flows. *Phys. Fluids* **32**, 080401 (2020).
59. Warsop, C. Current status and prospects for turbulent flow control. In *Aerodynamic Drag Reduction Technologies: Proceedings of the CEAS/DragNet European Drag Reduction Conference, 19–21 June 2000, Potsdam, Germany*, 269–277 (Springer, 2001).

60. Pollard, A. Passive and active control of near-wall turbulence. *Prog. Aerosp. Sci.* **33**, 689–708 (1998).
61. Sharma, A. & García-Mayoral, R. Turbulent flows over dense filament canopies. *J. Fluid Mech.* **888**, A2 (2020).
62. Luo, H. & Bewley, T. R. Design, modeling, and optimization of compliant tensegrity fabrics for the reduction of turbulent skin friction. In *Smart Structures and Materials 2003: Modeling, Signal Processing, and Control*, vol. 5049, 460–470 (SPIE, 2003).
63. Song, Q. et al. Tribological metamaterial: how feathers reduce drag and friction through hidden energy dissipation structures. *J. R. Soc. Interface* **22**, 20240751 (2025).
64. Hehner, M. T., Gatti, D. & Kriegseis, J. Stokes-layer formation under absence of moving parts—a novel oscillatory plasma actuator design for turbulent drag reduction. *Phys. Fluids* **31**, 051701 (2019).
65. Rosti, M. E., Brandt, L. & Pinelli, A. Turbulent channel flow over an anisotropic porous wall—drag increase and reduction. *J. Fluid Mech.* **842**, 381–394 (2018).
66. Dacome, G., Siebols, R. & Baars, W. Small-scale Helmholtz resonators with grazing turbulent boundary layer flow. *J. Turbulence* **25**, 461–481 (2024).
67. Hassanein, A., Modesti, D., Scarano, F. & Baars, W. J. Interaction of an inner-scaled Helmholtz resonator with boundary-layer turbulence. *Phys. Rev. Fluids* **9**, 114610 (2024).
68. Lin, C.-T., Ramakrishnan, V., Goza, A., Matlack, K. & Bae, J. Control for turbulent drag reduction by wall-normal blowing and suction. In *APS Division of Fluid Dynamics Meeting Abstracts*, L33–002 (2024).
69. Hickey, J.-P., Younes, K., Yao, M. X., Fan, D. & Muallem, J. Targeted turbulent structure control in wall-bounded flows via localized heating. *Phys. Fluids* **32**, 035104 (2020).
70. Zhu, S. et al. Controlling water waves with artificial structures. *Nat. Rev. Phys.* **6**, 231–245 (2024).
71. Bobinski, T., Maurel, A., Petitjeans, P. & Pagneux, V. Backscattering reduction for resonating obstacle in water-wave channel. *J. Fluid Mech.* <https://doi.org/10.1017/jfm.2018.302> (2018).
72. Bobinski, T., Eddi, A., Petitjeans, P., Maurel, A. & Pagneux, V. Experimental demonstration of epsilon-near-zero water waves focusing. *Appl. Phys. Lett.* <https://doi.org/10.1063/1.4926362> (2015).
73. Sharma, G. S., Skvortsov, A., MacGillivray, I. & Kessissoglou, N. On superscattering of sound waves by a lattice of disk-shaped cavities in a soft material. *Appl. Phys. Lett.* <https://doi.org/10.1063/1.5130695> (2020).
74. Berraquero, C. P., Maurel, A., Petitjeans, P. & Pagneux, V. Experimental realization of a water-wave metamaterial shifter. *Phys. Rev. E* <https://doi.org/10.1103/PhysRevE.88.051002> (2013).
75. Hu, X., Chan, C. T., Ho, K. M. & Zi, J. Negative effective gravity in water waves by periodic resonator arrays. *Phys. Rev. Lett.* <https://doi.org/10.1103/PhysRevLett.106.174501> (2011).
76. Hu, X., Yang, J., Zi, J., Chan, C. T. & Ho, K. M. Experimental observation of negative effective gravity in water waves. *Sci. Rep.* <https://doi.org/10.1038/srep01916> (2013).
77. Hu, X., Shen, Y., Liu, X., Fu, R. & Zi, J. Complete band gaps for liquid surface waves propagating over a periodically drilled bottom. *Phys. Rev. E* <https://doi.org/10.1103/PhysRevE.68.066308> (2003).
78. Kar, P., Sahoo, T. & Meylan, M. H. Bragg scattering of long waves by an array of floating flexible plates in the presence of multiple submerged trenches. *Phys. Fluids* <https://doi.org/10.1063/5.0017930> (2020).
79. Hu, X. & Chan, C. T. Refraction of water waves by periodic cylinder arrays. *Phys. Rev. Lett.* <https://doi.org/10.1103/PhysRevLett.95.154501> (2005).
80. Bennetts, L. G., Peter, M. A. & Craster, R. V. Graded resonator arrays for spatial frequency separation and amplification of water waves. *J. Fluid Mech.* <https://doi.org/10.1017/jfm.2018.648> (2018).
81. Wilks, B., Montiel, F. & Wakes, S. Rainbow reflection and broadband energy absorption of water waves by graded arrays of vertical barriers. *J. Fluid Mech.* <https://doi.org/10.1017/jfm.2022.302> (2022).
82. Archer, A. J. et al. Experimental realization of broadband control of water-wave-energy amplification in chirped arrays. *Phys. Rev. Fluids* <https://doi.org/10.1103/PhysRevFluids.5.062801> (2020).
83. De Vita, F., De Lillo, F., Bosia, F. & Onorato, M. Attenuating surface gravity waves with mechanical metamaterials. *Phys. Fluids* <https://doi.org/10.1063/5.0048613> (2021).
84. De Vita, F., De Lillo, F., Verzicco, R. & Onorato, M. A fully Eulerian solver for the simulation of multiphase flows with solid bodies: application to surface gravity waves. *J. Comput. Phys.* <https://doi.org/10.1016/j.jcp.2021.110355> (2021).
85. Palma, G., Mao, H., Burghignoli, L., Göransson, P. & Iemma, U. Acoustic metamaterials in aeronautics. *Appl. Sci.* **8**, 971 (2018).
86. Geyer, T. F., Sarradj, E. & Fritzsche, C. Porous airfoils: noise reduction and boundary layer effects. *Int. J. Aeroacoust.* **9**, 787–820 (2010).
87. Rubio Carpio, A. et al. Experimental characterization of the turbulent boundary layer over a porous trailing edge for noise abatement. *J. Sound Vib.* **443**, 537–558 (2019).
88. Teruna, C. et al. Noise reduction mechanisms of an open-cell metal-foam trailing edge. *J. Fluid Mech.* **898**, A18 (2020).
89. Teruna, C., Avallone, F., Casalino, D. & Ragni, D. Numerical investigation of leading edge noise reduction on a rod-airfoil configuration using porous materials and serrations. *J. Sound Vib.* **494**, 115880 (2021).
90. Jawahar, H., Karabasov, S. A. & Azarpeyvand, M. Jet installation noise reduction using porous treatments. *J. Sound Vib.* **545**, 117406 (2023).
91. Avallone, F., Ragni, D. & Casalino, D. Impingement of a propeller-slipstream on a leading edge with a flow-permeable insert: a computational aeroacoustic study. *Int. J. Aeroacoust.* **17**, 687–711 (2018).
92. Zamponi, R., Rubio Carpio, A., Avallone, F. & Ragni, D. Noise source analysis of porous fairings in a scaled landing gear model. *Aerosp. Sci. Technol.* **158**, 109885 (2025).
93. Shen, C., Xie, Y., Li, J., Cummer, S. A. & Jing, Y. Acoustic meta-cages for sound shielding with steady air flow. *J. Appl. Phys.* **123**, 124501 (2018).
94. Bilal, O. R., Ballagi, D. & Daraio, C. Architected lattices for simultaneous broadband attenuation of airborne sound and mechanical vibrations in all directions. *Phys. Rev. Appl.* **10**, 054060 (2018).
95. Guo, Y., Rosa, M. I. & Ruzzene, M. Topological surface states in a gyroid acoustic crystal. *Adv. Sci.* **10**, 2205723 (2023).
96. Kumar, S. & Lee, H. P. The present and future role of acoustic metamaterials for architectural and urban noise mitigations. In *Acoustics*, vol. 1, 590–607 (2019).
97. Ross, E. P., Figueroa-Ibrahim, K. M., Morris, S. C., L., S. D. & Bennett, G. J. Evaluating an additive manufactured acoustic metamaterial using the advanced noise control fan. *AIAA J.* **62**, 2783–2799 (2024).
98. Tek, M. Development of a generalized Darcy equation. *J. Pet. Technol.* **9**, 45–47 (1957).
99. Luesutthiviboon, S., Ragni, D., Avallone, F. & Snellen, M. An alternative permeable topology design space for trailing-edge noise attenuation. *Int. J. Aeroacoust.* **20**, 221–253 (2021).
100. Johnson, D. L., Koplik, J. & Dashen, R. Theory of dynamic permeability and tortuosity in fluid-saturated porous media. *J. Fluid Mech.* **176**, 379–402 (1987).
101. Iemma, U. & Palma, G. Design of metacontinua in the aeroacoustic spacetime. *Sci. Rep.* **10**, 18192 (2020).
102. Carpio, A. R., Avallone, F., Ragni, D., Snellen, M. & van der Zwaag, S. Quantitative criteria to design optimal permeable trailing edges for noise abatement. *J. Sound Vib.* **485**, 115596 (2020).

103. Zamponi, R., Avallone, F., Ragni, D., Schram, C. & Van Der Zwaag, S. Relevance of quadrupolar sound diffraction on flow-induced noise from porous-coated cylinders. *J. Sound Vib.* **583**, 118430 (2024).
104. Ingard, U. *Noise Reduction Analysis* (Jones & Bartlett Publishers, 2009).
105. Stewart, G. W. The tube as a branch of an acoustic conduct: the special case of the Quincke tube. *Phys. Rev.* **27**, 494–498 (1926).
106. Poirier, B., Maury, C. & Ville, J.-M. The use of Herschel–Quincke tubes to improve the efficiency of lined ducts. *Appl. Acoust.* **72**, 78–88 (2011).
107. Papathanasiou, T., Tsolakis, E., Spitas, V. & Movchan, A. The Herschel–Quincke tube with modulated branches. *Philos. Trans. R. Soc. A* **380**, 20220074 (2022).
108. Ko, S.-H. Sound attenuation in lined rectangular ducts with flow and its application to the reduction of aircraft engine noise. *J. Acoust. Soc. Am.* **50**, 1418–1432 (1971).
109. Arenas, J. P. & Crocker, M. J. Recent trends in porous sound-absorbing materials. *Sound Vib.* **44**, 12–18 (2010).
110. Zhen, N., Huang, R.-R., Fan, S.-W., Wang, Y.-F. & Wang, Y.-S. Resonance-based acoustic ventilated metamaterials for sound insulation. *npj Acoust.* **1**, 7 (2025).
111. Liang, Z. & Li, J. Extreme acoustic metamaterial by coiling up space. *Phys. Rev. Lett.* **108**, 114301 (2012).
112. Ghaffarivardavagh, R., Nikolaiczky, J., Anderson, S. & Zhang, X. Ultra-open acoustic metamaterial silencer based on fano-like interference. *Phys. Rev. B* **99**, 024302 (2019).
113. Sun, M., Fang, X., Mao, D., Wang, X. & Li, Y. Broadband acoustic ventilation barriers. *Phys. Rev. Appl.* **13**, 044028 (2020).
114. Tang, Y., Liang, B. & Lin, S. Broadband ventilated meta-barrier based on the synergy of mode superposition and consecutive fano resonances. *J. Acoust. Soc. Am.* **152**, 2412–2418 (2022).
115. Zhu, Y., Dong, R., Mao, D., Wang, X. & Li, Y. Nonlocal ventilating metasurfaces. *Phys. Rev. Appl.* **19**, 014067 (2023).
116. Liu, C., Xia, B. & Yu, D. The spiral-labyrinthine acoustic metamaterial by coiling up space. *Phys. Lett. A* **381**, 3112–3118 (2017).
117. Xiao, Z., Gao, P., Wang, D., He, X. & Wu, L. Ventilated metamaterials for broadband sound insulation and tunable transmission at low frequency. *Extrem. Mech. Lett.* **46**, 101348 (2021).
118. Chen, A., Zhao, X., Yang, Z., Anderson, S. & Zhang, X. Broadband labyrinthine acoustic insulator. *Phys. Rev. Appl.* **18**, 064057 (2022).
119. Lee, I., Han, I. & Yoon, G. Compact acoustic metamaterials based on azimuthal labyrinthine channels for broadband low-frequency soundproofing and ventilation. *Appl. Acoust.* **228**, 110273 (2025).
120. Liu, C. et al. Three-dimensional soundproof acoustic metacage. *Phys. Rev. Lett.* **127**, 084301 (2021).
121. Krasikova, M. et al. Metahouse: noise-insulating chamber based on periodic structures. *Adv. Mater. Technol.* **8**, 2200711 (2023).
122. Meng, Y. et al. Subwavelength broadband perfect absorption for unidimensional open-duct problems. *Adv. Mater. Technol.* **8**, 2201909 (2023).
123. Yang, Z., Chen, A., Xie, X., Anderson, S. W. & Zhang, X. Phase gradient ultra open metamaterials for broadband acoustic silencing. *Sci. Rep.* **15**, 21434 (2025).
124. Yang, M., Chen, S., Fu, C. & Sheng, P. Optimal sound-absorbing structures. *Mater. Horiz.* **4**, 673–680 (2017).
125. Li, X., Zhang, H., Tian, H., Huang, Y. & Wang, L. Frequency-tunable sound insulation via a reconfigurable and ventilated acoustic metamaterial. *J. Phys. D* **55**, 495108 (2022).
126. Wen, G. et al. Origami-based acoustic metamaterial for tunable and broadband sound attenuation. *Int. J. Mech. Sci.* **239**, 107872 (2023).
127. Jones, M. G., Watson, W. R. & Parrott, T. L. Benchmark data for evaluation of aeroacoustic propagation codes with grazing flow. *AIAA Pap.* **2853**, 2005 (2005).
128. Bonomo, L. A. et al. A Comparison of Impedance Eduction Test Rigs with Different Flow Profiles. <https://doi.org/10.2514/6.2023-3346>.
129. Aurégan, Y. & Leroux, M. Experimental evidence of an instability over an impedance wall in a duct with flow. *J. Sound Vib.* **317**, 432–439 (2008).
130. Zheng, M., Chen, C. & Li, X. Experimental investigation of factors influencing acoustic liner drag using direct measurement. *Aerosp. Sci. Technol.* **130**, 107903 (2022).
131. Minotti, A., Simon, F. & Gantié, F. Characterization of an acoustic liner by means of Laser Doppler Velocimetry in a subsonic flow. *Aerosp. Sci. Technol.* **12**, 398–407 (2008).
132. Quintino, N. T. et al. Comparison of impedance eduction test rigs with different boundary-layer profiles. *AIAA J.* <https://doi.org/10.2514/1.J065173> (2025).
133. Howerton, B. M. & G., M. A conventional liner acoustic drag interaction benchmark database. *23rd AIAA/CEAS Aeroacoustics Conference* <https://doi.org/10.2514/6.2017-4190>.
134. Jasinski, C. & Corke, T. Mechanism for increased viscous drag over porous sheet acoustic liners. *AIAA J.* **58**, 3393–3404 (2020).
135. Shuaizhong Zhang, P. O., Ye, W. & den Toonder, J. A concise review of microfluidic particle manipulation methods. *Microfluidics Nanofluidics* **24**, 20 (2020).
136. Godary, T. et al. Acoustofluidics: technology advances and applications from 2022 to 2024. *Anal. Chem.* **97**, 24 (2025).
137. Ding, X. et al. Surface acoustic wave microfluidics. *Lab a Chip* **13**, 3626–3649 (2016).
138. Guo, F. et al. Three-dimensional manipulation of single cells using surface acoustic waves. *Proc. Natl. Acad. Sci. USA* **113**, 1522–1527 (2016).
139. Wu, M. et al. Acoustofluidic separation of cells and particles. *Microsyst. Nanoeng.* **5**, 18 (2019).
140. Shen, L. et al. Acousto-dielectric tweezers enable independent manipulation of multiple particles. *Sci. Adv.* **10**, 10 (2024).
141. Bruus, H. Acoustofluidics 7: The acoustic radiation force on small particles. *Lab a Chip* **12**, 1014–1021 (2013).
142. Cesewski, E. et al. Additive manufacturing of three-dimensional (3D) microfluidic-based microelectromechanical systems (MEMS) for acoustofluidic applications. *Lab a Chip* **18**, 2087–2098 (2018).
143. Li, F. et al. Phononic-crystal-enabled dynamic manipulation of microparticles and cells in an acoustofluidic channel. *Phys. Rev. Appl.* **13**, 044077 (2020).
144. Huang, L. et al. Phononic crystal-induced standing Lamb wave for the translation of subwavelength microparticles. *Appl. Phys. Lett.* **121**, 023505 (2022).
145. Zeighami, F. et al. Elastic metasurfaces for Scholte-Stoney wave control. *Philos. Trans. R. Soc. A* **382**, 20230365 (2024).
146. Surappa, S. et al. Dynamically reconfigurable acoustofluidic metasurface for subwavelength particle manipulation and assembly. *Nat. Commun.* **16**, 1–10 (2025).
147. Charara, M., Kujala, Z., Lee, S. & Gonella, S. Spatially selective drop-motion programming using metamaterials. In *Proceedings A*, vol. 481, 20240429 (The Royal Society, 2025).
148. Caleap, M. & Drinkwater, B. W. Acoustically trapped colloidal crystals that are reconfigurable in real time. *Proc. Natl. Acad. Sci. USA* **111**, 6226–6230 (2014).
149. Kadic, M., Milton, G. W., van Hecke, M. & Wegener, M. 3D metamaterials. *Nat. Rev. Phys.* **1**, 198–210 (2019).
150. Jin, Y. et al. The 2024 phononic crystals roadmap. *J. Phys. D* **58**, 113001 (2025).
151. Chen, Y., Frenzel, T., Guenneau, S., Kadic, M. & Wegener, M. Mapping acoustical activity in 3D chiral mechanical metamaterials onto micropolar continuum elasticity. *J. Mech. Phys. Solids* **137**, 103877 (2020).

152. Chen, Y., Kadic, M. & Wegener, M. Roton-like acoustical dispersion relations in 3D metamaterials. *Nat. Commun.* **12**, 3278 (2021).
153. Craster, R., Guenneau, S., Kadic, M. & Wegener, M. Mechanical metamaterials. *Rep. Prog. Phys.* **86**, 094501 (2023).
154. Chen, Y., Fleury, R., Seppecher, P., Hu, G. & Wegener, M. Nonlocal metamaterials and metasurfaces. *Nat. Rev. Phys.* **7**, 299–312 (2025).
155. Nassar, H. et al. Nonreciprocity in acoustic and elastic materials. *Nat. Rev. Mater.* **5**, 667–685 (2020).
156. Chen, Y. et al. High-frequency gravitational-wave detection using a chiral resonant mechanical element and a short unstable optical cavity. Preprint at *arXiv* <https://doi.org/10.48550/arXiv.2007.07974> (2020).
157. Cummer, S. A., Christensen, J. & Alù, A. Controlling sound with acoustic metamaterials. *Nat. Rev. Mater.* **1**, 1–13 (2016).
158. Qu, J., Kadic, M. & Wegener, M. Three-dimensional poroelastic metamaterials with extremely negative or positive effective static volume compressibility. *Extrem. Mech. Lett.* **22**, 165–171 (2018).
159. Zhang, S.-Y., Yan, D.-J., Wang, Y.-S., Wang, Y.-F. & Laude, V. Wave propagation in one-dimensional fluid-saturated porous phononic crystals with partial-open pore interfaces. *Int. J. Mech. Sci.* **195**, 106227 (2021).
160. Fleury, R., Khanikaev, A. B. & Alù, A. Floquet topological insulators for sound. *Nat. Commun.* **7**, 11744 (2016).
161. Huber, S. D. Topological mechanics. *Nat. Phys.* **12**, 621–623 (2016).
162. Khanikaev, A. B. et al. Photonic topological insulators. *Nat. Mater.* **12**, 233–239 (2013).
163. Wang, P., Lu, L. & Bertoldi, K. Topological phononic crystals with one-way elastic edge waves. *Phys. Rev. Lett.* **115**, 104302 (2015).
164. Serra-Garcia, M. et al. Observation of a phononic quadrupole topological insulator. *Nature* **555**, 342–345 (2018).
165. Ma, G., Xiao, M. & Chan, C. T. Topological phases in acoustic and mechanical systems. *Nat. Rev. Phys.* **1**, 281–294 (2019).
166. Berry, M. V. Quantal phase factors accompanying adiabatic changes. *Proc. R. Soc. Lond.* <https://doi.org/10.1098/rspa.1984.0023> (1984).
167. Zak, J. Berry's phase for energy bands in solids. *Phys. Rev. Lett.* **62**, 2747 (1989).
168. Jiang, W. et al. Topological band evolution between Lieb and kagome lattices. *Phys. Rev. B* **99**, 125131 (2019).
169. Martínez, J. A. I., Laforge, N., Kadic, M. & Laude, V. Topological waves guided by a glide-reflection symmetric crystal interface. *Phys. Rev. B* **106**, 0643041 (2022).
170. Ponti, J. M. D. et al. Localized topological states beyond Fano resonances via counter-propagating wave mode conversion in piezoelectric microelectromechanical devices. *Nat. Commun.* **15**, 9617 (2024).
171. Xue, H., Yang, Y., Gao, F., Chong, Y. & Zhang, B. Acoustic higher-order topological insulator on a kagome lattice. *Nat. Mater.* **18**, 108–112 (2019).
172. Ni, X., Weiner, M., Alù, A. & Khanikaev, A. B. Observation of higher-order topological acoustic states protected by generalized chiral symmetry. *Nat. Mater.* **18**, 113–120 (2019).
173. Luo, L. et al. Observation of a phononic higher-order Weyl semimetal. *Nat. Mater.* **20**, 794–799 (2021).
174. Ma, Q. et al. Observation of higher-order nodal-line semimetal in phononic crystals. *Phys. Rev. Lett.* **132**, 066601 (2024).
175. Yang, Z. et al. Topological acoustics. *Phys. Rev. Lett.* **114**, 114301 (2015).
176. Lu, J., Qiu, C., Ke, M. & Liu, Z. Valley vortex states in sonic crystals. *Phys. Rev. Lett.* **116**, 093901 (2016).
177. Lu, J. et al. Observation of topological valley transport of sound in sonic crystals. *Nat. Phys.* **13**, 369–374 (2017).
178. Zhang, X., Xiao, M., Cheng, Y., Lu, M.-H. & Christensen, J. Topological sound. *Commun. Phys.* **1**, 97 (2018).
179. Laforge, N. et al. Observation of topological gravity-capillary waves in a water wave crystal. *N. J. Phys.* **21**, 083031 (2019).
180. Makwana, M. P. et al. Experimental observations of topologically guided water waves within non-hexagonal structures. *Applied Physics Letters* **116** (2020).
181. Laforge, N. et al. Acoustic topological circuitry in square and rectangular phononic crystals. *Phys. Rev. Appl.* **15**, 054056 (2021).
182. Wu, X. et al. Topological phononics arising from fluid-solid interactions. *Nat. Commun.* **13**, 6120 (2022).
183. Zhao, S. et al. Topological acoustofluidics. *Nat. Mater.* **24**, 707–715 (2025).
184. Samak, M. M. & Bilal, O. R. Direct observation of all-flat bands phononic metamaterials. *Phys. Rev. Lett.* **133**, 266101 (2024).
185. Eringen, A. C. & Wegner, J. Nonlocal continuum field theories. *Appl. Mech. Rev.* **56**, B20–B22 (2003).
186. Landau, L. D. et al. *Electrodynamics of continuous media*, vol. 8 (elsevier, 2013).
187. Krushynska, A. A. & Meleshko, V. V. Normal waves in elastic bars of rectangular cross section. *J. Acoust. Soc. Am.* **129**, 1324–1335 (2011).
188. Chen, Y. et al. Anomalous frozen evanescent phonons. *Nat. Commun.* **15**, 8882 (2024).
189. Iglesias Martínez, J. A., Chen, Y., Wang, K. & Wegener, M. Nonlocal conduction in a metawire. *Adv. Mater.* **37**, 2415278 (2025).
190. Iglesias Martínez, J. A. et al. Experimental observation of roton-like dispersion relations in metamaterials. *Sci. Adv.* **7**, eabm2189 (2021).
191. Wang, K., Chen, Y., Kadic, M., Wang, C. & Wegener, M. Nonlocal interaction engineering of 2D roton-like dispersion relations in acoustic and mechanical metamaterials. *Commun. Mater.* **3**, 35 (2022).
192. Kazemi, A. et al. Drawing dispersion curves: band structure customization via nonlocal phononic crystals. *Phys. Rev. Lett.* **131**, 176101 (2023).
193. Fleury, R., Sounas, D. L., Sieck, C. F., Haberman, M. R. & Alù, A. Sound isolation and giant linear nonreciprocity in a compact acoustic circulator. *Science* **343**, 516–519 (2014).
194. Goldsberry, B. M., Wallen, S. P. & Haberman, M. R. Nonreciprocity and mode conversion in a spatiotemporally modulated elastic wave circulator. *Phys. Rev. Appl.* **17**, 034050 (2022).
195. Galiffi, E. et al. Photonics of time-varying media. *Adv. Photonics* **4**, 014002–014002 (2022).
196. Palermo, A., Celli, P., Yousefzadeh, B., Daraio, C. & Marzani, A. Surface wave non-reciprocity via time-modulated metamaterials. *J. Mech. Phys. Solids* **145**, 104181 (2020).
197. Torrent, D., Poncelet, O. & Batsale, J.-C. Nonreciprocal thermal material by spatiotemporal modulation. *Phys. Rev. Lett.* **120**, 125501 (2018).
198. Kang, J. & Haberman, M. R. Sound diffusion with spatiotemporally modulated acoustic metasurfaces. *Appl. Phys. Lett.* <https://doi.org/10.1063/5.0097590> (2022).
199. Goldsberry, B. M., Norris, A. N., Wallen, S. P. & Haberman, M. R. Green's function approach to model vibrations of beams with spatiotemporally modulated properties. *Proc. R. Soc. A* <https://doi.org/10.1098/rspa.2024.0580> (2025).
200. Farhat, M., Guenneau, S., Chen, P.-Y. & Wu, Y. Spacetime modulation in floating thin elastic plates. *Phys. Rev. B* **104**, 014308 (2021).
201. Koukouraki, M., Petitjeans, P., Maurel, A. & Pagneux, V. Floquet scattering of shallow water waves by a vertically oscillating plate. *Wave Motion* <https://doi.org/10.2139/ssrn.5055878> (2024).
202. Cassidy, E. & Oliner, A. Dispersion relations in time-space periodic media: Part i—Stable interactions. *Proc. IEEE* **51**, 1342–1359 (1963).
203. Tessier Brothelande, S. et al. Experimental evidence of non-reciprocal propagation in space-time modulated piezoelectric

- phononic crystals. *Appl. Phys. Lett.* <https://doi.org/10.1063/5.0169265> (2023).
204. Harwood, A. C. et al. Space-time optical diffraction from synthetic motion. *Nat. Commun.* **16**, 5147 (2025).
  205. Nassar, H., Xu, X., Norris, A. & Huang, G. Modulated phononic crystals: Non-reciprocal wave propagation and Willis materials. *J. Mech. Phys. Solids* **101**, 10–29 (2017).
  206. Huidobro, P., Silveirinha, M., Galiffi, E. & Pendry, J. Homogenization theory of space-time metamaterials. *Phys. Rev. Appl.* **16**, 014044 (2021).
  207. Touboul, M., Lombard, B., Assier, R. C., Guenneau, S. & Craster, R. V. High-order homogenization of the time-modulated wave equation: non-reciprocity for a single varying parameter. *Proc. R. Soc. A* <https://doi.org/10.1098/rspa.2023.0776> (2024).
  208. Zhu, X. et al. Tunable unidirectional compact acoustic amplifier via space-time modulated membranes. *Phys. Rev. B* **102**, 024309 (2020).
  209. Tirole, R. et al. Second harmonic generation at a time-varying interface. *Nat. Commun.* <https://doi.org/10.1038/s41467-024-51588-z> (2024).
  210. Santini, J., Pu, X., Palermo, A., Braghin, F. & Riva, E. Controlling surface acoustic waves (SAWs) via temporally graded metasurfaces. *J. Sound Vib.* **592**, 118632 (2024).
  211. Ammari, H., Cao, J., Hiltunen, E. O. & Rueff, L. Scattering from time-modulated subwavelength resonators. *Proc. R. Soc. A* <https://doi.org/10.1098/rspa.2024.0177> (2024).
  212. Taravati, S. & Eleftheriades, G. V. Microwave space-time-modulated metasurfaces. *ACS Photonics* **9**, 305–318 (2022).
  213. Norris, A. Acoustic cloaking theory. *Proc. R. Soc. A* **464**, 2411–2434 (2008).
  214. Visser, M. Acoustic propagation in fluids: an unexpected example of Lorentzian geometry. Preprint at *arXiv* <https://doi.org/10.48550/arXiv.gr-qc/9311028> (1993).
  215. Garcia-Meca, C. et al. Analogue transformations in physics and their application to acoustics. *Sci. Rep.* **3**, 2009–2014 (2013).
  216. Carrol, S. *Spacetime and Geometry—An Introduction to General Relativity* (Cambridge University Press, Cambridge, 2019).
  217. Colombo, G., Palma, G. & Iemma, U. Numerical aeroacoustic assessment of a metacontinuum device impinged by a laser-generated sound source. *J. Eng.* **2024**, 1–11 (2024).
  218. Colombo, G. & Iemma, U. Assessment of the performances and limitations of spacetime convective corrections for acoustic metacontinua design. *Sci. Rep.* **15**, 1–12 (2025).
  219. Collis, S. S., Joslin, R. D., Seifert, A. & Theofilis, V. Issues in active flow control: theory, control, simulation, and experiment. *Prog. Aerosp. Sci.* **40**, 237–289 (2004).
  220. Brunton, S. L. & Noack, B. R. Closed-loop turbulence control: progress and challenges. *Appl. Mech. Rev.* **67**, 050801 (2015).
  221. Bilal, O. R., Süssstrunk, R., Daraio, C. & Huber, S. D. Intrinsically polar elastic metamaterials. *Adv. Mater.* **29**, 1700540 (2017).
  222. Mao, X. & Lubensky, T. C. Maxwell lattices and topological mechanics. *Annu. Rev. Condens. Matter Phys.* **9**, 413–433 (2018).
  223. Charara, M., McInerney, J., Sun, K., Mao, X. & Gonella, S. Omnidirectional topological polarization of bilayer networks: analysis in the Maxwell limit and experiments on a 3d-printed prototype. *Proc. Natl. Acad. Sci.* **119**, e2208051119 (2022).
  224. Walsh, M. & Weinstein, L. Drag and heat transfer on surfaces with small longitudinal fins. In *11th Fluid and Plasma Dynamics Conference*, 1161 (1978).
  225. Fedorov, A. V., Malmuth, N. D., Rasheed, A. & Hornung, H. G. Stabilization of hypersonic boundary layers by porous coatings. *AIAA J.* **39**, 605–610 (2001).
  226. Liu, Z. et al. Locally resonant sonic materials. *science* **289**, 1734–1736 (2000).
  227. Van Buren, T., Floryan, D., Ding, L., Hellström, L. & Smits, A. Turbulent pipe flow response to a step change in surface roughness. *J. Fluid Mech.* **904**, A38 (2020).
  228. Li, Y., Jiang, X., Liang, B., Cheng, J.-C. & Zhang, L. Metascreen-based acoustic passive phased array. *Phys. Rev. Appl.* **4**, 024003 (2015).
  229. Cheng, Y. et al. Ultra-sparse metasurface for high reflection of low-frequency sound based on artificial Mie resonances. *Nat. Mater.* **14**, 1013–1019 (2015).
  230. Frenzel, T. et al. Three-dimensional labyrinthine acoustic metamaterials. *Appl. Phys. Lett.* **103**, 061907 (2013).

## Acknowledgements

The authors acknowledge EUROMECH 659 “Metamaterials in Fluid Flows, Aeroacoustics, and beyond” held in Groningen, The Netherlands, on 25–28 March 2025, as a driving event for this work. Mu.K. acknowledges support by the EIPHI Graduate School, ANR OPTOBOT (Contract No. ANR-17-EURE-0002) and ANR PNanoBot (Contract No. ANR-21-CE33-0015). M.W. acknowledges support by Deutsche Forschungsgemeinschaft through the Excellence Cluster “3D Matter Made to Order” (EXC 2082/2). A.O.K. acknowledges financial support by the Dutch Research Council (NWO) through the “MetaFlow” project (KICH1.ST04.22.010) for organizing the Euromech659 event. R.V.C. is supported by the H2020 FET-proactive Metamaterial Enabled Vibration Energy Harvesting (MetaVEH) project under Grant Agreement No. 952039. RVC is also funded by UK Research and Innovation (UKRI) and EPSRC through grant number EP/Y015673/1. Ma.K. acknowledges support by the European Research Council (ERC, MetaWing, 16762850) and the Dutch Research Council NWO-I (OCENW.M20.186). M.R.H. acknowledges support from the Office of Naval Research under Award No. N00014-23-1-2660. M.I.H. acknowledges the Office of Naval Research Multidisciplinary University Research Initiative (MURI) Grant Number N0001421268. F.A. is co-funded by the European Union (ERC, LINING, 101075903). However, views and opinions expressed are those of the authors alone and do not necessarily reflect those of the European Union or the European Research Council. Neither the European Union nor the granting authority can be held responsible for them.

## Author contributions

All authors wrote and reviewed the paper.

## Competing interests

The authors declare no competing interests.

## Additional information

**Correspondence** and requests for materials should be addressed to Muamer Kadic or Anastasiia O. Krushynska.

**Peer review information** *Nature Communications* thanks Osama Bilal, Claus Claeys, and Lei Xu, who co-reviewed with Xiangying Shen, for their contribution to the peer review of this work.

**Reprints and permissions information** is available at <http://www.nature.com/reprints>

**Publisher’s note** Springer Nature remains neutral with regard to jurisdictional claims in published maps and institutional affiliations.

**Open Access** This article is licensed under a Creative Commons Attribution-NonCommercial-NoDerivatives 4.0 International License, which permits any non-commercial use, sharing, distribution and reproduction in any medium or format, as long as you give appropriate credit to the original author(s) and the source, provide a link to the Creative Commons licence, and indicate if you modified the licensed material. You do not have permission under this licence to share adapted material derived from this article or parts of it. The images or other third party material in this article are included in the article's Creative Commons licence, unless indicated otherwise in a credit line to the material. If material is not included in the article's Creative Commons licence and your intended use is not permitted by statutory regulation or exceeds the permitted use, you will need to obtain permission directly from the copyright holder. To view a copy of this licence, visit <http://creativecommons.org/licenses/by-nc-nd/4.0/>.

© The Author(s) 2026

---

<sup>1</sup>Politecnico di Torino, Department of Mechanical and Aerospace Engineering, Torino, Italy. <sup>2</sup>Politecnico di Torino, Department of Applied Science and Technology, Torino, Italy. <sup>3</sup>Institute of Applied Physics and Institute of Nanotechnology, Karlsruhe Institute of Technology (KIT), Karlsruhe, Germany. <sup>4</sup>Roma Tre University, Department of Civil, Computer Science and Aeronautical Technologies Engineering, Rome, Italy. <sup>5</sup>UMI 2004 Abraham de Moivre-CNRS, Imperial College London, London, UK. <sup>6</sup>Politecnico di Milano, Department of Civil and Environmental Engineering, Milan, Italy. <sup>7</sup>DAAA, ONERA, Institut Polytechnique de Paris, Châtillon, France. <sup>8</sup>The University of Texas at Austin, Walker Department of Mechanical Engineering, Austin, TX, USA. <sup>9</sup>University of Colorado Boulder, Smead Department of Aerospace Engineering Sciences, Boulder, CO, USA. <sup>10</sup>Seoul National University, Department of Mechanical Engineering, Seoul, Republic of Korea. <sup>11</sup>Air Force Research Laboratory, Wright-Patterson AFB, OH, USA. <sup>12</sup>Université Marie et Louis Pasteur, CNRS, Institut FEMTO-ST, Besançon, France. <sup>13</sup>Delft University of Technology, Faculty of Aerospace Engineering, Delft, The Netherlands. <sup>14</sup>DAAA, ONERA, Institut Polytechnique de Paris, Meudon, France. <sup>15</sup>DMPE, ONERA, Université de Toulouse, Toulouse, France. <sup>16</sup>University at Buffalo (SUNY), Department of Mechanical and Aerospace Engineering, Buffalo, NY, USA. <sup>17</sup>POEMS, ENSTA, CNRS, INRIA, Institut Polytechnique de Paris, Palaiseau, France. <sup>18</sup>University of Groningen, Faculty of Science and Engineering, Groningen, The Netherlands. ✉e-mail: [muamer.kadic@univ-fcomte.fr](mailto:muamer.kadic@univ-fcomte.fr); [a.o.krushynska@rug.nl](mailto:a.o.krushynska@rug.nl)